

UCSF

UC San Francisco Electronic Theses and Dissertations

Title

Artificial activation of the DNA replication checkpoint and 11 new substrates of the beta-TRCP ubiquitin ligase

Permalink

<https://escholarship.org/uc/item/09s756t8>

Author

Loveless, Theresa Berens

Publication Date

2015

Peer reviewed|Thesis/dissertation

Artificial activation of the DNA replication checkpoint and 11 new
substrates of the beta-TRCP ubiquitin ligase

by

Theresa Berens Loveless

DISSERTATION

Submitted in partial satisfaction of the requirements for the degree of

DOCTOR OF PHILOSOPHY

in

Cell Biology

in the

GRADUATE DIVISION

of the

UNIVERSITY OF CALIFORNIA, SAN FRANCISCO

Copyright 2015

By

Theresa Berens

Loveless

ACKNOWLEDGEMENTS

First, I would like to thank my advisor, David Toczyski, for his mentorship and support throughout my Ph.D. work, and for conceiving and guiding these projects. Thank you to all the members of the Toczyski Lab for their help and advice during these projects, most importantly Shastyn Galaang, Ben Topacio, and Katie Ulrich. For moral support, I thank all my labmates (I tried to list you individually but it was everyone – the T lab is a really special place); my thesis committee, Nevan Krogan, Joachim Li, and Martin McMahon; classmates, especially Anna Reade, Joshua Dunn, Anna Payne-Tobin Jost, Hayley Pemble, Vanessa van Voorhis, Laura Yee, Kelly Nissen, and Michael Todhunter; housemates Brian Rodriguez and Govind Persad; and finally my parents, Matthew and Eileen Berens; and siblings Sean Berens, Bryan Berens, Andrew Berens, Laura Berens, Sarette Albin, Anna Gunderson, Ian Loveless, and Bri Butler. Most importantly, for their infinite patience, I thank my husband Matthew Loveless and son Virgil Loveless.

STATEMENT REGARDING AUTHOR CONTRIBUTIONS

Chapter two is a reprint on a *Molecular Biology of the Cell* article published in 2012 (volume 23, number 6) by me and my advisor, David P. Toczyski. We designed the experiments and wrote the paper, and I performed all the experiments.

Chapter three is a reprint of a *PLoS Genetics* article published in 2015 (volume 11, issue 6) by me, Benjamin R. Topacio, Ajay A. Vashisht, Shastyn Galaang, Katie M. Ulrich, Brian D. Young, James A. Wohlschlegel, and David P. Toczyski. Ajay A. Vashisht, Brian D. Young, and James A. Wohlschlegel performed, directed, or analyzed all the mass spectrometry experiments. Along with David P. Toczyski, I designed and directed all other experiments, and performed, with some assistance, the experiments in figures 4-6.

Artificial activation of the DNA replication checkpoint and 11 new substrates of the beta-TRCP ubiquitin ligase

Theresa Berens Loveless

When DNA is damaged, or DNA replication goes awry, cells activate checkpoints to allow time for damage to be repaired and replication to complete. In *Saccharomyces cerevisiae*, the DNA damage checkpoint, which responds to lesions such as double-strand breaks, is activated when the lesion promotes the association of the sensor kinase Mec1 and its targeting subunit Ddc2 with its activators Ddc1 (a member of the 9-1-1 complex) and Dpb11. It has been more difficult to determine what role these Mec1 activators play in the replication checkpoint, which recognizes stalled replication forks, since Dpb11 has a separate role in DNA replication itself. Therefore, we constructed an *in vivo* replication-checkpoint mimic, which recapitulates Mec1-dependent phosphorylation of the effector kinase Rad53, a crucial step in checkpoint activation. In the natural replication checkpoint, Mec1 phosphorylation of Rad53 requires Mrc1, a replisome component. The replication-checkpoint mimic requires co-localization of Mrc1-Lacl and Ddc2-Lacl, and is independent of both Ddc1 and Dpb11. We show that these activators are also dispensable for Mec1 activity and cell survival in the natural replication checkpoint, but that Ddc1 is absolutely required in the absence of Mrc1. We propose that co-localization of Mrc1 and Mec1 is the minimal signal required to activate the replication checkpoint.

The Skp1-Cul1-F box complex (SCF) associates with any one of a number of F box proteins, which serve as substrate binding adaptors. The human F box protein β TRCP directs the conjugation of ubiquitin to a variety of substrate proteins, leading to the destruction of the substrate by the proteasome. To identify β TRCP substrates, we employed a recently-developed technique, called Ligase Trapping, wherein a ubiquitin ligase is fused to a ubiquitin-

binding domain to “trap” ubiquitinated substrates. 88% of the candidate substrates that we examined were bona fide substrates, comprising twelve previously validated substrates, eleven new substrates and three false positives. One β TRCP substrate, CReP, is a Protein Phosphatase 1 (PP1) specificity subunit that targets the translation initiation factor eIF2 α to promote the removal of a stress-induced inhibitory phosphorylation and increase cap-dependent translation. We found that CReP is targeted by β TRCP for degradation upon DNA damage. Using a stable CReP allele, we show that depletion of CReP is required for the full induction of eIF2 α phosphorylation upon DNA damage, and contributes to keeping the levels of translation low as cells recover from DNA damage.

TABLE OF CONTENTS

Title Page	i
Acknowledgements	iii
Statement regarding author contributions	iv
Abstract	v
Table of Contents	vii
List of Figures	viii
Chapter One	1
Introduction	
Chapter Two	2
Co-localization of Mec1 and Mrc1 is sufficient for Rad53 phosphorylation <i>in vivo</i>	
Chapter Three	41
DNA damage regulates translation through β -TRCP targeting of CReP	

LIST OF FIGURES

Chapter Two

- Figure 1. Co-localization of Mec1-Ddc2 and Mrc1 promotes Rad53 phosphorylation independent of Ddc1 and Dpb11. 26
- Figure 2. The replication-checkpoint mimic faithfully reproduces qualities of the replication checkpoint. 27
- Figure 3. Rad53 can be phosphorylated in response to replication stress in the absence of 9-1-1 and Dpb11. 28
- Figure 4. Rad53 phosphorylation in the absence of 9-1-1 requires Mrc1. 29
- Table 1. Yeast strains used in this study. 30
- Figure S1. *dpb11-1* cells cannot grow at 34°C 37
- Figure S2. Rad53 can be activated in response to replication stress in the absence of 9-1-1 and Dpb11. 38
- Figure S3. Rad53 phosphorylation in the absence of 9-1-1 requires Mrc1. 39
- Figure S4. Rad53 activation in response to MMS is equivalent in *ddc1Δ tel1Δ* and *ddc1Δ dpb11-1* mutants. 40

Chapter Three

- Table 1. Discovery and validation summary for identified β TRCP substrates. 46
- Figure 1. Establishing Ligase Trapping in human cells. 71
- Figure 2. Validation of novel β TRCP substrates. 72
- Figure 3. Ubiquitin ligase binding and turnover of a subset of novel β TRCP substrates. 73
- Figure 4. CReP ubiquitination is dependent on CRLs and turnover is regulated by a β TRCP consensus degron. 74
- Figure 5. Regulation of CReP turnover and impact on eIF2 α phosphorylation. 76

Figure 6. Consequences of CReP turnover downstream of eIF2 α phosphorylation.	78
Figure S1: Development of the mammalian Ligase Trapping protocol.	80
Figure S2: Purification of ubiquitinated β -catenin by the β TRCP Ligase Trap.	81
Figure S3: Conservation of degrons observed in candidate β TRCP substrates.	82
Figure S4: Pulldown of ubiquitinated species of candidate substrates by the β TRCP Ligase Trap.	83
Figure S5: Pulldown of ubiquitinated species of candidate substrates by the β TRCP Ligase Trap.	84
Figure S6: Determination of candidate substrate stability and effect of SCF inhibition.	85
Figure S7: Effect of MG132 on β TRCP Ligase Trap pulldowns.	86
Figure S8: Accumulation of CReP upon CRL inhibition.	87
Figure S9: Phospho-site mapping of CReP.	88
Figure S10: Amino acid sequence of CReP, with stabilizing mutations marked.	90
Figure S11: DNA damage decreases CReP half-life.	91
Figure S12: CRL activity is required for full CReP depletion and eIF2 α phosphorylation after UV treatment in mouse embryonic fibroblasts (MEFs).	91

Chapter 1: Summary Introduction

Previous work had shown that yeast cells recognize DNA damage, and activate appropriate checkpoint signaling, when two proteins are independently recruited to the site of damage: the sensor kinase Mec1 and the Mec1 activator Ddc1. Artificially co-localizing these two proteins was shown to be sufficient to activate checkpoint signaling, primarily through phosphorylation of the effector kinase Rad53. In Chapter 2, I used a similar artificial co-localization system to show that Mec1 can phosphorylate Rad53 in the absence of its known activators as long as it is co-localized with the replication fork protein Mrc1. Consistently, I also found that checkpoint activation during DNA replication did not require the known Mec1 activators.

Ubiquitin ligases are often important signaling proteins, which act by conjugating the small protein ubiquitin to their specific substrates. Therefore, there has been much interest in methods to identify ubiquitin ligase substrates. One common method is to immunoprecipitate ubiquitin ligases and identify their interactors by mass spectrometry, some of which will be substrates. Previous work in yeast had improved on these methods by fusing the ubiquitin ligase to an ubiquitin binding domain. In Chapter 3, I describe the adaptation of this method to human cells, and use it to identify 11 new substrates of the ubiquitin ligase β TRCP. One of these substrates, CReP, is depleted after DNA damage, and this depletion contributes to the inhibition of the translation machinery.

Chapter 2:

Co-localization of Mec1 and Mrc1 is sufficient for Rad53 phosphorylation *in vivo*

Theresa J. Berens* and David P. Toczyski*†

*Department of Biochemistry and Biophysics, University of California, San Francisco

1450 3rd St. HD350, San Francisco, CA 94131

†Correspondence: toczyski@cc.ucsf.edu

Running head: Mec1 activation in a replication-checkpoint mimic

Abstract

When DNA is damaged, or DNA replication goes awry, cells activate checkpoints to allow time for damage to be repaired and replication to complete. In *Saccharomyces cerevisiae*, the DNA damage checkpoint, which responds to lesions such as double-strand breaks, is activated when the lesion promotes the association of the sensor kinase Mec1 and its targeting subunit Ddc2 with its activators Ddc1 (a member of the 9-1-1 complex) and Dpb11. It has been more difficult to determine what role these Mec1 activators play in the replication checkpoint, which recognizes stalled replication forks, since Dpb11 has a separate role in DNA replication itself. Therefore, we constructed an *in vivo* replication-checkpoint mimic, which recapitulates Mec1-dependent phosphorylation of the effector kinase Rad53, a crucial step in checkpoint activation. In the natural replication checkpoint, Mec1 phosphorylation of Rad53 requires Mrc1, a replisome component. The replication-checkpoint mimic requires co-localization of Mrc1-LacI and Ddc2-LacI, and is independent of both Ddc1 and Dpb11. We show that these activators are also dispensable for Mec1 activity and cell survival in the natural replication checkpoint, but that Ddc1 is absolutely required in the absence of Mrc1. We propose that co-localization of Mrc1 and Mec1 is the minimal signal required to activate the replication checkpoint.

Introduction

To avoid passing on damaged DNA, cells activate checkpoints under conditions that threaten the genome. The better-studied of the DNA integrity checkpoints, the DNA damage checkpoint, is activated when initial processing of a wide variety of DNA lesions reveals stretches of single-stranded DNA (Garvik *et al.*, 1995; Lee *et al.*, 1998). In *Saccharomyces cerevisiae*, the mechanism by which this DNA structure activates checkpoint signaling has been well-delineated: RPA-coated single-stranded DNA recruits the sensor kinase Mec1 through its binding partner, Ddc2 (Rouse and Jackson, 2002; Zou and Elledge, 2003; Ball *et al.*, 2004), while the junction between RPA-coated single-stranded and double-stranded DNA independently (Edwards *et al.*, 1999; Melo *et al.*, 2001) recruits the 9-1-1 clamp (Majka and Burgers, 2003; Zou *et al.*, 2003; Ellison and Stillman, 2003; Majka *et al.*, 2006a). Ddc1, a subunit of 9-1-1, then increases the kinase activity of Mec1 both directly and by recruiting Dpb11, another Mec1 activator (Majka *et al.*, 2006b; Mordes *et al.*, 2008; Navadgi-Patil and Burgers, 2008; Navadgi-Patil and Burgers, 2009). Mec1 phosphorylates histone H2A, creating a mark referred to as gamma-H2A, which is the correlate of the mark made on the metazoan

H2A variant H2AX (Downs *et al.*, 2000; Downs *et al.*, 2004). Along with a constitutive methylation on H3K79, gamma-H2A promotes the recruitment of Rad9, the checkpoint mediator (Nakamura *et al.*, 2004; Huyen *et al.*, 2004; Giannattasio *et al.*, 2005). Alternatively, Rad9 can be recruited by a 9-1-1-Dpb11 complex (Saka *et al.*, 1997; Furuya *et al.*, 2004; Puddu *et al.*, 2008; Pfander and Diffley, 2011). Rad9 phosphorylation by Mec1 promotes Rad9's association with the checkpoint effector kinase Rad53, which binds these Rad9 phosphorylations through its FHA domains (Emili, 1998; Sun *et al.*, 1998; Vialard *et al.*, 1998; Schwartz *et al.*, 2002). This is thought to position Rad53 for Mec1 phosphorylation (Sweeney *et al.*, 2005), leading to Rad53 autophosphorylation and activation (Gilbert *et al.*, 2001; Usui *et al.*, 2009). Activated Rad53 can then diffuse away from the site of damage and phosphorylate downstream effectors of the checkpoint. Tel1, a sensor kinase related to Mec1, can perform some of the same activities as Mec1. Tel1 phosphorylates and activates Rad53 using the mediator Rad9 (P. Garber and D.P.T., unpublished results). However, Tel1 does not require activation by Ddc1 or Dpb11 (Giannattasio *et al.*, 2002; reviewed in Mordes and Cortez, 2008).

The DNA replication checkpoint uses much of the same machinery as the DNA damage checkpoint. However, it responds to stalled replication forks during S phase (reviewed in Tourrière and Pasero, 2007). Both canonical Mec1 activators Ddc1 and Dpb11 may play a role in the replication checkpoint (Wang and Elledge, 2002), although it is not clear if they are absolutely required (Navadgi-Patil and Burgers, 2009; Puddu *et al.*, 2011). Mec1 is recruited to stalled replication forks, probably through an interaction with RPA-coated single-stranded DNA (Osborn and Elledge, 2003; Katou *et al.*, 2003). A significant difference between the replication checkpoint and the DNA damage checkpoint is that a different mediator protein is used. Rad9 does not appear to participate in the replication checkpoint; instead, Mrc1 acts as the checkpoint mediator (Alcasabas *et al.*, 2001). Mrc1 is part of the replication machinery and travels with replication forks during every S phase, and therefore does not need to be specifically recruited to stalled replication forks (Osborn and Elledge, 2003). On fork stalling,

Mec1 phosphorylates Mrc1, which promotes the recruitment and activation of Rad53 (Osborn and Elledge, 2003). As in the DNA damage checkpoint, active Rad53 leads to arrest of the cell cycle at mitosis, destruction of the ribonucleotide reductase inhibitor Sml1, and transcriptional regulation (reviewed in Tourrière and Pasero, 2007). However, these activities of Rad53 are less important for cell survival after acute, as opposed to chronic, replication stress. Rad53 also stabilizes stalled replication forks so that they can restart efficiently after replication stress is over, in part by blocking the activity of Exo1 (Segurado and Diffley, 2008). This fork stabilization is the checkpoint function essential for cell survival after acute replication stress (Desany *et al.*, 1998; Tercero *et al.*, 2003).

In vitro experiments using purified proteins demonstrate that Dpb11 and Ddc1 activate Mec1 directly (Majka *et al.*, 2006b; Mordes *et al.*, 2008; Navadgi-Patil and Burgers, 2008). Additionally, artificial co-localization of Ddc1 and Mec1 on chromatin promotes Mec1 activity *in vivo* (Bonilla *et al.*, 2008). This co-localization was achieved through a system in which an array of *lac* operator repeats (LacO) was integrated into the genome and Ddc1 and the Mec1 binding partner Ddc2 were fused to *lac* repressor (LacI). Ddc2-LacI was used instead of directly tethering Mec1 to LacI, since C-terminal Mec1 fusions are not functional. Co-localization of Ddc1 and Ddc2 LacI fusions promoted phosphorylation of Rad9 and Rad53, and cell cycle arrest.

We used a similar approach to investigate Mec1 activation in the replication checkpoint. We fused Ddc2 and Mrc1 to LacI and showed that this replication-checkpoint mimic can promote phosphorylation of Rad53. The Mec1 activator Dpb11 has an essential role in the initiation of DNA replication, confounding attempts to examine its checkpoint signaling role in isolation. Because the replication-checkpoint mimic enacts checkpoint signaling in the absence of DNA replication, it provides an ideal setting in which to examine Dpb11's role in Mec1 activation. We show that Mec1 activity in the replication-checkpoint mimic does not depend on Dpb11 or Ddc1. Furthermore Mec1 can act through Mrc1 to phosphorylate Rad53 in the natural

replication checkpoint, even in a *ddc1 dpb11-1* strain, and that activity is sufficient to maintain viability after acute replication stress. Therefore, we propose that, whereas Ddc1 and Dpb11 aid in replication checkpoint activation, co-localization of Mec1 and Mrc1 at stalled replication forks promotes Rad53 activation sufficient to stabilize the replisome during transient replication stress.

Results

Development of a replication-checkpoint mimic

Co-localization of Mec1 and the 9-1-1 complex through the induction of Ddc2-GFP-Lacl and Ddc1-GFP-Lacl promotes phosphorylation of Rad53 in the absence of DNA damage. This is dependent on Rad9 (Bonilla *et al.*, 2008, and Figure 1A), since Mrc1 is not recruited to the LacO array. To generate a mimic of the replication checkpoint, we fused Mrc1 to GFP Lacl. Mrc1-GFP-Lacl (hereafter referred to as Mrc1-Lacl) can substitute for Rad9 and allow Rad53 phosphorylation in a strain lacking Rad9 (Figure 1A). Importantly, this replication-checkpoint mimic signaling was assayed in nocodazole-arrested cells, so it is independent of DNA replication and of S phase.

Recruitment of Rad9 is mediated by histone modifications. Therefore, even though Ddc1-Lacl and Ddc2-Lacl are able to associate through dimerization of Lacl (and possibly GFP), this is not sufficient for Rad9 activation and a LacO array is required. In contrast, Rad53 phosphorylation mediated by Mrc1-Lacl should not require chromatin. Therefore, we determined whether the LacO array was required for activation of the replication-checkpoint mimic. While activation of this replication-checkpoint mimic was enhanced by integration of an array of LacO, Rad53 was partially phosphorylated in a strain without a LacO array (Figure 1A). Next we tested whether all three Lacl fusions were required for checkpoint activation (Figure 1B). As expected, neither Mrc1-Lacl alone nor Mrc1-Lacl/Ddc1-Lacl promoted Rad53

phosphorylation. However, co-localization of just Mrc1-Lacl and Ddc2-Lacl was sufficient to promote Rad53 phosphorylation without Ddc1-Lacl.

Mec1 activators in the replication-checkpoint mimic

Having shown that the Lacl fusion of the Mec1-activating 9-1-1 component Ddc1 was not required for the replication-checkpoint mimic, we tested whether Ddc1 or the other known Mec1 activator, Dpb11, were required at all. We could not delete *DPB11* because it is essential for DNA replication. *In vitro* studies have shown that the Mec1-activating domain of Dpb11 lies at the C-terminus, between amino acids 572 and 764 (Mordes *et al.*, 2008; Navadgi-Patil and Burgers, 2008). The protein encoded by *dpb11-1* is truncated after amino acid 582. Although *dpb11-1* has been reported to have checkpoint defects (Araki *et al.*, 1995; Wang and Elledge, 2002; Puddu *et al.*, 2011), it is formally possible that the 11 amino acids between 572 and 582 could partially activate Mec1, especially since similarly-sized domains of Ddc1 have been shown to activate Mec1 (Navadgi-Patil and Burgers, 2009). Therefore, we tested the activity of the replication-checkpoint mimic in the *dpb11-1 ddc1Δ* mutant at 34°C, a non-permissive temperature for *dpb11-1* (Supplementary Figure S1). Rad53 is phosphorylated as strongly in the *ddc1Δ dpb11-1* strain as in a *DDC1 DPB11* strain (Figure 1C). Thus we conclude that neither Ddc1 nor Dpb11 is required for activity of the replication-checkpoint mimic.

Optimization and further characterization of the replication-checkpoint mimic

As shown in Figure 1B, the Ddc2-Lacl/Mrc1-Lacl system phosphorylated Rad53 less efficiently than the original Ddc1-Lacl/Ddc2-Lacl DNA-damage checkpoint mimic. We hypothesized that this resulted from low expression of Mrc1-Lacl relative to Ddc2-Lacl (see Figures 1A and B). Therefore, we expressed Mrc1-Lacl from a stronger promoter (Gal instead of GalS), such that its levels are almost as high as Ddc2-Lacl. This resulted in more robust Rad53 phosphorylation (unpublished data and Figure 2A).

In this optimized replication-checkpoint mimic, again, neither Mrc1-Lacl nor Ddc2-Lacl alone is sufficient to activate Rad53. Deletion of *RAD9* or *DDC1* in the mimic strain did not have

a strong impact on Rad53 phosphorylation (Figure 2A). It is likely that Ddc1 cannot be recruited to the LacO array, since there is no junction between ds and ssDNA, and therefore it is not surprising that the status of the 9-1-1 complex is not important. Rad9 is not phosphorylated in response to stalled replication forks in an *MRC1* wildtype strain (Alcasabas *et al.*, 2001), so this feature of the replication-checkpoint mimic matches the natural checkpoint. However, it is unclear why Rad9 cannot be recruited to either a natural stalled replication fork or the LacO array in our system; we investigate this question further in Figure 4. In this optimized system, as in Figure 1A, some Rad53 phosphorylation was seen in the absence of the LacO array.

Most of the Mrc1 in cells is associated with the proteins Csm3 and Tof1. Both Csm3 and Tof1 are required for normal localization of Mrc1 to replication forks (Katou *et al.*, 2003; Bando *et al.*, 2009), and *tof1* Δ cells cannot activate the replication checkpoint (Foss, 2001). However, *csm3* Δ and *tof1* Δ cells activated the replication-checkpoint mimic as efficiently as wildtype cells (Figure 2B), suggesting that these proteins play no direct role in the replication checkpoint, and that the checkpoint defects observed when they are mutated are the result of mis-localization of Mrc1.

In the endogenous replication checkpoint, phosphorylation of Mrc1 by Mec1 is required to recruit Rad53 and promote its phosphorylation. Therefore, the *mrc1*^{AQ} mutant protein, in which all potential Mec1 phosphorylation sites are removed, cannot promote Rad53 phosphorylation (Osborn and Elledge, 2003). In agreement with this, *mrc1*^{AQ}-LacI could not promote Rad53 phosphorylation in the replication-checkpoint mimic (Figure 2C). The *mrc1*^{AQ}-LacI protein could be non-specifically hypomorphic, for example by being partially unfolded. Therefore, we screened for integrants expressing higher levels of *mrc1*^{AQ}-LacI, and showed that these also failed to phosphorylate Rad53 (Figure 2C, fourth strain).

Mec1 activity during replication stress

Since Mec1 phosphorylation of Rad53 in the replication-checkpoint mimic did not depend on known Mec1 activators, we tested whether these activators were required during

replication stress induced by treatment with the ribonucleotide reductase inhibitor hydroxyurea (HU) for four hours at 23°C. To make sure we observed Mec1 activity only, we deleted the *MEC1* ortholog *TEL1*. Rad53 phosphorylation in response to HU treatment was reduced when *DDC1* was deleted, but only slightly more reduced when *dpb11-1* was also introduced (Figure 3A). Consistent with what we observed in the replication-checkpoint mimic, the *ddc1Δ dpb11-1 tel1Δ* strain still displayed significant Rad53 phosphorylation upon HU treatment, while, as expected, a *mec1Δ tel1Δ* mutant did not phosphorylate Rad53 (Figure 3A). Levels of Rad53 phosphorylation in these mutants observed by gel shift (Figure 3A) were recapitulated when the same samples were tested for Rad53 kinase activity by in situ assay (Supplemental Figure S2). This is consistent with both the replication checkpoint and the minimal endogenous checkpoint relying exclusively on Mec1 and Mrc1, although unknown proteins could be required in both cases, since these experiments are performed *in vivo*.

To test the physiological relevance of the levels of Rad53 phosphorylation we observed in these mutants, we treated them with HU for four and six hours at 23°C, then washed out the drug and plated cells on rich medium to test viability (Figure 3B). Wildtype cells, and all single and double mutants of *ddc1Δ*, *tel1Δ*, and *dpb11-1*, retained >75% viability after HU treatment. Similarly the *ddc1Δ dpb11-1 tel1Δ* triple mutant retained about 50% viability, as compared to an almost complete loss of viability in *mec1Δ tel1Δ* strains, which lack all checkpoint signaling.

Previous studies showed that Mec1-dependent Rad53 phosphorylation requires *DDC1* in cells arrested in G1 with alpha factor or in mitosis with nocodazole (Paciotti *et al.*, 1998; Navadgi-Patil and Burgers, 2009). Therefore, we tested whether Ddc1-independent phosphorylation of Rad53 by Mec1 depended on Mrc1, which is active only in S phase. An *mrc1Δ ddc1Δ tel1Δ* strain could not phosphorylate Rad53, suggesting that 9-1-1 is required for Rad9-mediated Rad53 phosphorylation but not Mrc1-mediated Rad53 phosphorylation (Figure 4A) or activity (Supplemental Figure S3). Consistently, this triple mutant cannot survive a 2.5 hr. treatment with HU at 30°C (Figure 4B). As expected, inactivation of 9-1-1 by deletion of the

clamp loader *RAD24* gives the same result as deletion of *DDC1* (Figure 4C), consistent with an earlier observation in a *TEL1* strain (Bjergbaek *et al.*, 2005).

The slightly increased Rad53 phosphorylation observed when *MRC1* is deleted in a *tel1Δ* strain is consistent with a report that *mrc1Δ* strains phosphorylate Rad53 even in the absence of replication-stressing agents such as HU, likely because Mrc1 has a checkpoint-independent role in promoting replisome stability (Alcasabas *et al.*, 2001).

The requirement for Mrc1 in the absence of 9-1-1 suggested that the other checkpoint mediator, Rad9, cannot function for some reason at stalled replication forks or in the absence of 9-1-1. One possibility is that 9-1-1 is physically required for recruitment or function of Rad9. When Rad9 is recruited to the site of DNA damage, it is phosphorylated by Mec1. Then it mediates Rad53 autophosphorylation and is phosphorylated by Rad53 in the process. Therefore we tested whether Rad9 could be phosphorylated in various mutants (Figure 4D). For these experiments, we used methyl methanesulfonate (MMS) instead of HU, since Rad9 is not phosphorylated upon HU treatment in *MRC1* strains. It is not surprising that both Rad53 and Rad9 are robustly phosphorylated in wild-type or *tel1Δ*. However, in MMS, Rad53 phosphorylation is even more significantly reduced in all *ddc1Δ* strains than it was in HU (Figure 4D). This is unsurprising since checkpoint signaling in HU depends most on Mrc1 (and thus is independent of Ddc1), whereas signaling in MMS is more dependent on Rad9 (Alcasabas *et al.*, 2001; Komata *et al.*, 2009). The levels of Rad53 phosphorylation (Figure 4D) and activity (Supplemental Figure S4) are comparable in the *ddc1Δtel1Δ* and *ddc1Δ dpb11-1* strains, but levels of Rad9 phosphorylation vary significantly. Rad9 exhibits no phospho shift in *ddc1Δtel1Δ* and a striking shift in *ddc1Δ dpb11-1*. We know that Rad9 activity is not absolutely dependent on Tel1, since the *mrc1Δ tel1Δ* strain can still phosphorylate Rad53 (Figure 4A). Therefore we conclude that phosphorylation of Rad9 requires either Tel1 or Mec1 and Ddc1, reinforcing the idea that the activation of Mec1 by 9-1-1 is critical for Rad9- but not Mrc1-mediated activity.

Discussion

Here we report Mec1-dependent Rad53 phosphorylation in the absence of the canonical Mec1 activators Ddc1 and Dpb11, both in response to replication stress and in an artificial in vivo system. The essential role of Dpb11 in replication limits the ability to examine its role in the replication checkpoint. We eliminated this issue by using a replication-checkpoint mimic, which allows us to assay Mrc1-dependent checkpoint activation outside of S phase. Others reported that Rad53 phosphorylation in a *ddc1Δ dpb11-1* strain is restricted to S phase ([Navadgi-Patil and Burgers, 2009](#); [Puddu et al., 2011](#)). To show that this represented Mec1 activity in the absence of its activators, we demonstrated Rad53 phosphorylation in a *ddc1Δ dpb11-1 tel1Δ* strain. Our results also suggest the mechanism by which activator-independent Mec1 activity is restricted to S phase: in the absence of Ddc1, phosphorylation of Rad53 is absolutely dependent on Mrc1, the S-phase-specific checkpoint mediator that is a constitutive part of the DNA replisome ([Figure 4](#)). Furthermore, forced colocalization of Mec1 and Mrc1 is sufficient to phosphorylate Rad53 in metaphase-arrested cells undergoing neither DNA replication nor DNA damage ([Figure 1](#)). We propose that a high local concentration of Mrc1, both at a stalled replication fork and in the replication-checkpoint mimic, allows unactivated Mec1 to phosphorylate Mrc1, which leads to Rad53 recruitment and a high local concentration of Rad53, allowing unactivated Mec1 to phosphorylate Rad53. Alternatively, an undiscovered, replication-specific Mec1 activator could operate at stalled replication forks. Of importance, the Rad53 phosphorylation we observe is sufficient to promote survival of acute replication stress ([Figure 3B](#)). Here we place our results in the context of the extensive literature showing replication checkpoint defects in *dpb11-1* and *ddc1Δ dpb11-1* strains, outline the molecular events implied by our results and model, and suggest likely cellular consequences of the Mec1-dependent, activator-independent Rad53 phosphorylation we observe.

We propose that the replication-checkpoint phenotypes associated with *dpb11-1* and *ddc1Δ dpb11-1* strains can be understood as a function of the dual role of Dpb11 in promoting DNA replication initiation and checkpoint signaling or of the difference between levels of Rad53 activation required for growth under chronic replication stress and levels sufficient for survival of acute replication stress. Dpb11 was first implicated in checkpoint signaling because *dpb11-1* cells, which are incompetent for DNA replication at the restrictive temperature, fail to arrest in mitosis when exposed to replication stress, even at the permissive temperature (Araki et al., 1995). At the restrictive temperature, *dpb11-1* cells could not phosphorylate Rad53 in response to replication stress (Wang and Elledge, 1999). Later Mordes et al. (2008) and Navadgi-Patil and Burgers (2008) showed that the product of *dpb11-1* is a truncation that lacks almost all of the domain required for Mec1 activation. The phenotypes of *dpb11-1* certainly reflect some genuine defect in Rad53 phosphorylation in *dpb11-1* cells. However, impairment of replication initiation can nonspecifically prevent activity of the replication checkpoint by reducing the number of replication forks, even if the mutated protein does not participate directly in checkpoint signaling (Shimada et al., 2002). *dpb11-1* cells have defective replication initiation at the permissive and restrictive temperatures (Kamimura et al., 1998). Therefore the replication-checkpoint phenotypes of *dpb11-1* probably reflect a combination of defective replication initiation and defective checkpoint signaling. We avoided this conflation by using the replication-checkpoint mimic, which does not require the replication function of Dpb11, to show that neither Dpb11 nor Ddc1 is required for Mec1 phosphorylation of Rad53.

The phenotypes of *ddc1Δ dpb11-1* double mutants likely also reflect the high level of Rad53 phosphorylation required to grow in the presence of chronic replication stress. It was proposed that Ddc1 and Dpb11 act independently to promote Mec1 activation in response to replication stress, because either single mutant can grow well in the presence of hydroxyurea but the double mutant cannot (Wang and Elledge, 2002). Furthermore, Ddc1 and Dpb11 can

activate Mec1 independently of each other (Navadgi-Patil and Burgers, 2009). Puattu et al. (2011) showed that Rad53 phosphorylation in a *ddc1Δ dpb11-1* strain is insufficient to allow growth under chronic replication stress, but this level of Rad53 phosphorylation can promote cell survival after acute replication stress. Because they did not observe Rad53 phosphorylation in a *ddc1Δ dpb11-1 tel1Δ* triple mutant, they attributed Rad53 phosphorylation in the *ddc1Δ dpb11-1* strain to Tel1. We do see Rad53 phosphorylation in the *ddc1Δ dpb11-1 tel1Δ* strain. Moreover, our *ddc1Δ dpb11-1 tel1Δ* cells can survive acute replication stress two orders of magnitude better than *mec1Δ tel1Δ* cells, indicating that Mec1 must have significant function remaining in the absence of activation by Ddc1 and Dpb11.

The unique structure of a stalled replication fork, as opposed to a processed double-strand break or other lesion, may explain why checkpoint signaling can be activated in the *ddc1Δ dpb11-1 tel1Δ* strain by HU treatment during S phase but not outside of S phase. Mec1 is recruited to stalled forks, whereas Mrc1 is already present (Osborn and Elledge, 2003; Katou et al., 2003). If colocalization of Mec1 and Mrc1 is the only requirement for the reduced but significant level of checkpoint activation we observe in the *ddc1Δ dpb11-1 tel1Δ* strain, then Mec1 recruitment to a stalled fork is the only molecular event required to activate the checkpoint. In vitro results suggest that this model is possible, since Mrc1 purified from bacteria can promote Mec1 phosphorylation of Rad53 even in the absence of Mec1 activators (Chen and Zhou, 2009). Moreover, some Rad53 phosphorylation is seen in the replication-checkpoint mimic in the absence of a LacO array, suggesting that the Ddc2-LacI/Mrc1-LacI heterodimer is sufficient to promote Rad53 phosphorylation (Figures 1A and 2A). Alternatively, if a replication-specific activator of Mec1 exists and is required for all Mec1 phosphorylation of Rad53, our replication-checkpoint mimic results suggest that 1) it must be recruited by either Mrc1 or Mec1-Ddc2, 2) it does not require that Mec1-Ddc2 be bound to chromatin, and 3) it does not depend on 9-1-1, Dpb11, Tof1, or Csm3.

The ability of Mrc1, but not the other checkpoint mediator, Rad9, to promote 9-1-1-independent Mec1 phosphorylation of Rad53 is probably explained in one of two ways: Mrc1 could be a better Mec1 substrate, either intrinsically or because it is present at a high local concentration at stalled forks, or Rad9 might not be recruited to stalled replication forks in the absence of 9-1-1 and Tel1. Indeed, we found that Rad9 could not be phosphorylated in response to MMS unless either 9-1-1 or Tel1 was intact ([Figure 4C](#)). Consistent with this, a recent article shows that the 9-1-1–Dpb11 complex is one pathway by which Rad9 can be recruited to Mec1 ([Pfander and Diffley, 2011](#)).

DNA integrity checkpoints protect the genome in four ways: by arresting the cell cycle until damage can be repaired or replication can complete, changing transcription to promote DNA repair and cell-cycle arrest, inhibiting late-origin firing, and acting at stalled replication forks to stabilize them. This last activity is the only one required for survival of acute replication stress, and it may occur locally at the stalled fork that activated the checkpoint. [Puddu et al. \(2011\)](#) showed that some of the other checkpoint readouts may be impaired in *ddc1Δ dpb11-1* mutants, but survival of acute replication stress is not impaired. We showed significant survival in the *ddc1Δ dpb11-1 tel1Δ* strain. Perhaps the Mec1 phosphorylation of Rad53 that we observe in this strain provides, in wild-type cells, a way to stabilize transiently stalled forks without engaging the entire checkpoint machinery

Methods

Yeast strains

For complete genotypes, see Table 1. All strains are from the W303-1a background (*rad5* mutation uncorrected). LacI fusions were integrated at the marker locus, while Rad53 was tagged at its endogenous locus. For strains containing LacO arrays, array length was

measured by Southern blot. Genomic DNA was digested with *Bgl*II and probed with the *Xba*I fragment of pAFS52, which contains the LacO repeat. All Mrc1-LacI strains within the same experiment have the same array length, and the length is noted in the genotype. Rad9 was tagged with a PCR fragment containing appropriate homology, the 3xFlag tag, and the gene for hygromycin B resistance. *MEC1*, *TEL1*, and *RAD24* were disrupted with the *TRP1* sequence. In replication-checkpoint mimic strains, *DDC1* was deleted with a *URA3* cassette that was subsequently looped out, while *RAD9* was deleted by transformation with a PCR fragment containing appropriate homology and the hygromycin B resistance gene. In other TBY strains, *DDC1*, *MRC1*, and *RAD9* were deleted by transformation with a PCR fragment containing appropriate homology and genes for resistance to G418, nourseothricin, and hygromycin B, respectively. In PGY strains, *RAD9* was disrupted with *HIS3* and *MRC1* was disrupted with *g418^R*.

Activation of replication-checkpoint mimic

All experiments were performed at 30°C except that shown in Figure 1C, which is described below. Cells were grown to late log phase in YM1+2% dextrose, collected and resuspended in YM1+2% raffinose, and grown for two hours. Nocodazole was added to 10µg/mL and cells were arrested for three hours. 0.75 OD₆₀₀ were collected and flash-frozen on dry ice for the “0 hr.” timepoint. Then, 2% galactose was added to promote transcription of the LacI fusions and cells were grown for a further hour, at which point 2% dextrose was added to shut off transcription. Further timepoints were collected at 3 hr. and 5 hr. after galactose addition.

For Figure 1C, the protocol was as above, except the initial parts of the experiment were performed at 23°C. After three hours arrest in nocodazole, cells were moved to 34°C for an additional hour before addition of galactose.

Treatment with hydroxyurea (HU) and methyl methanesulfonate (MMS)

Experiments for Figures 3 and 4D were performed at 22.5°C, while experiments for Figure 4A-C were performed at 30°C. To cells in early log phase were added 0.2 M HU (Sigma #H8627), 0.05% MMS (Acros Organics # 156890050), or medium alone. For western blotting, cells were incubated in medium alone for 2.5 hours (Figures 3 and 4D) or 1.5 hours (Figure 4A and C) and in HU or MMS for 4 hours (Figures 3 and 4D), 2.5 hours (4A) or 2.8 hours (4C). Then, pellets equivalent to an OD₆₀₀ of 0.75 were collected and flash-frozen on dry ice.

For viability experiments, the same volume of cells for a given strain was plated before HU treatment and after 4 and 6 hours HU at 22.5°C (Figure 3B) or 2.5 hours HU at 30°C (Figure 4B). Colonies were counted and the number at 4 and 6 hours was divided by the number at 0 hours to give the fraction of viable cells.

Western blotting and antibodies

Cell pellets were lysed in 20% trichloroacetic acid with glass beads, and protein was precipitated and resuspended in SDS sample buffer. SDS-PAGE gels to be blotted for Rad53-HA or Rad9-3xFlag were Tris-HCl 6% acrylamide (37.5:1). All other gels were Criterion Tris-HCl 4-20% gradients (BioRad #345-0034). Rad53-HA was detected with 1:1,000 mouse monoclonal anti-HA 16B12 (Covance # MMS-101P), for Figures 1C, 2B-C, 3, and 4, or 1:2,000 rabbit anti-Rad53 (DAB001, kind gift of D. Durocher), for Figures 1A-B and 2A. Rad9-3xFlag was detected with 1:1,000 mouse monoclonal anti-Flag M2 (Sigma #F3165), X-GFP-LacI fusions with 1:1,000 mouse monoclonal anti-GFP JL-8 (Clontech #632380), and Cdc28 with 1:1,000 goat anti-Cdc28 yC-20 (Santa Cruz #sc-6709).

Acknowledgements

We thank H. Araki for the *dpb11-1* mutant, D. Durocher for the anti-Rad53 antibody, and Nevan Krogan, Joachim Li, and members of the Toczyski lab for helpful conversations. This work was funded by NIH grant GMO59691 to D.P.T.

References

Alcasabas, A.A., Osborn, A.J., Bachant, J., Hu, F., Werler, P.J., Bousset, K., Furuya, K., Diffley, J.F., Carr, A.M., Elledge, S.J. (2001). Mrc1 transduces signals of DNA replication stress to activate Rad53. *Nat.Cell.Biol.* 11:958-65.

Araki, H., Leem, S.H., Phongdara, A., Sugino, A. (1995). Dpb11, which interacts with DNA polymerase II(epsilon) in *Saccharomyces cerevisiae*, has a dual role in S-phase progression and at a cell cycle checkpoint. *Proc.Natl.Acad.Sci.USA.* 92(25):11791-5.

Ball, H.L., Myers, J.S., Cortez, D. (2005). ATRIP binding to replication protein A-single-stranded DNA promotes ATR-ATRIP localization but is dispensable for Chk1 phosphorylation. *Mol.Biol.Cell.* 16(5):2372-81.

Bando, M., Katou, Y., Komata, M., Tanaka, H., Itoh, T., Sutani, T., Shirahige, K. (2009). Csm3, Tof1, and Mrc1 form a heterotrimeric mediator complex that associates with DNA replication forks. *J.Biol.Chem.* 284(49):34355-65.

Bjergbaek, L., Cobb, J.A., Tsai-Pflugfelder, M., Gasser, S.M. (2005). Mechanistically distinct roles for Sgs1p in checkpoint activation and replication fork maintenance. *EMBO J.* 2005 Jan 26;24(2):405-17.

Bonilla, C.Y., Melo, J.A., Toczyski, D.P. (2008). Colocalization of sensors is sufficient to activate the DNA damage checkpoint in the absence of damage. *Mol.Cell.* 30(3):267-76.

Chen, S.H., Zhou, H. (2009). Reconstitution of Rad53 activation by Mec1 through adaptor protein Mrc1. *J.Biol.Chem.* 284(28):18593-604.

Desany, B.A., Alcasabas, A.A., Bachant, J.B., Elledge, S.J. (1998). Recovery from DNA replicational stress is the essential function of the S-phase checkpoint pathway. *Genes.Dev.* 12(18):2956-70.

.

Downs, J.A., Allard, S., Jobin-Robitaille, O., Javaheri, A., Auger, A., Bouchard, N., Kron, S.J., Jackson, S.P., Côté, J. (2004). Binding of chromatin-modifying activities to phosphorylated histone H2A at DNA damage sites. *Mol.Cell.* 16(6):979-90.

Downs, J.A., Lowndes, N.F., Jackson, S.P. (2000). A role for *Saccharomyces cerevisiae* histone H2A in DNA repair. *Nature.* 408(6815):1001-4.

Edwards, R.J., Bentley, N.J., Carr, A.M. (1999). A Rad3-Rad26 complex responds to DNA damage independently of other checkpoint proteins. *Nat.Cell.Biol.* 1(7):393-8.

Ellison, V., Stillman, B. (2003). Biochemical characterization of DNA damage checkpoint complexes: clamp loader and clamp complexes with specificity for 5' recessed DNA. *PLoS.Biol.* 1(2):E33.

Emili, A. (1998). MEC1-dependent phosphorylation of Rad9p in response to DNA damage. *Mol.Cell.* 2(2):183-9.

Foss, E.J. (2001) Tof1p regulates DNA damage responses during S phase in *Saccharomyces cerevisiae*. *Genetics.* 157(2):567-77.

Furuya, K., Poitelea, M., Guo, L., Caspari, T., Carr, A.M. (2004). Chk1 activation requires Rad9 S/TQ-site phosphorylation to promote association with C-terminal BRCT domains of Rad4TOPBP1. *Genes Dev.* 18(10):1154-64.

Garvik, B., Carson, M., Hartwell, L. (1995). Single-stranded DNA arising at telomeres in *cdc13* mutants may constitute a specific signal for the RAD9 checkpoint. *Mol.Cell.Biol.* 15(11):6128-38.

Giannattasio, M., Sommariva, E., Vercillo, R., Lippi-Boncambi, F., Liberi, G., Foiani, M., Plevani, P., Muzi-Falconi, M.. (2002). A dominant-negative MEC3 mutant uncovers new functions for the Rad17 complex and Tel1. *Proc.Natl.Acad.Sci.USA.* 99(20):12997-3002.

Giannattasio M, Lazzaro F, Plevani P, Muzi-Falconi M. (2005). The DNA damage checkpoint response requires histone H2B ubiquitination by Rad6-Bre1 and H3 methylation by Dot1. *J.Biol.Chem.* 280(11):9879-86.

Gilbert, C.S., Green, C.M., Lowndes, N.F. (2001). Budding yeast Rad9 is an ATP-dependent Rad53 activating machine. *Mol.Cell.* 8(1):129-36.

Huyen, Y., Zgheib, O., Ditullio, R.A. Jr., Gorgoulis, V.G., Zacharatos, P., Petty, T.J., Sheston, E.A., Mellert, H.S., Stavridi, E.S., Halazonetis, T.D. (2004) Methylated lysine 79 of histone H3 targets 53BP1 to DNA double-strand breaks. *Nature*. 432(7015):406-11.

Kamimura, Y., Masumoto, H., Sugino, A., Araki, H. (1998). Sld2, which interacts with Dpb11 in *Saccharomyces cerevisiae*, is required for chromosomal DNA replication. *Mol.Cell.Biol.* 18(10):6102-9.

Katou, Y., Kanoh, Y., Bando, M., Noguchi, H., Tanaka, H., Ashikari, T., Sugimoto, K., Shirahige, K. (2003). S-phase checkpoint proteins Tof1 and Mrc1 form a stable replication-pausing complex. *Nature*. 424(6952):1078-83.

Komata, M., Bando, M., Araki, H., Shirahige, K. (2009). The direct binding of Mrc1, a checkpoint mediator, to Mcm6, a replication helicase, is essential for the replication checkpoint against methyl methanesulfonate-induced stress. *Mol.Cell.Biol.* 18:5008-19.

Lee, S.E., Moore, J.K., Holmes, A., Umezū, K., Kolodner, R.D., Haber, J.E. (1998). *Saccharomyces* Ku70, mre11/rad50 and RPA proteins regulate adaptation to G2/M arrest after DNA damage. *Cell*. 94(3):399-409.

Majka, J., Binz, S.K., Wold, M.S., Burgers, P.M. (2006a). Replication protein A directs loading of the DNA damage checkpoint clamp to 5'-DNA junctions. *J.Biol.Chem.* 281(38):27855-61.

Majka, J., Burgers, P.M. (2003). Yeast Rad17/Mec3/Ddc1: a sliding clamp for the DNA damage checkpoint. *Proc.Natl.Acad.Sci.USA*. 100(5):2249-54.

Majka, J., Niedziela-Majka, A., Burgers, P.M. (2006b). The checkpoint clamp activates Mec1 kinase during initiation of the DNA damage checkpoint. *Mol.Cell*. 24(6):891-901.

Melo, J.A., Cohen, J., Toczyski, D.P. (2001). Two checkpoint complexes are independently recruited to sites of DNA damage in vivo. *Genes.Dev*. 15(21):2809-21.

Mordes, D.A., Cortez, D. (2008). Activation of ATR and related PIKKs. *Cell.Cycle*. 7(18):2809-12.

Mordes, D.A., Nam, E.A., Cortez, D. (2008). Dpb11 activates the Mec1-Ddc2 complex. *Proc.Natl.Acad.Sci.USA*. 105(48):18730-4.

Nakamura, T.M., Du, L.L., Redon, C., Russell, P. (2004). Histone H2A phosphorylation controls Crb2 recruitment at DNA breaks, maintains checkpoint arrest, and influences DNA repair in fission yeast. *Mol.Cell.Biol*. 14:6215-30.

Navadgi-Patil, V.M., Burgers, P.M. (2008). Yeast DNA replication protein Dpb11 activates the Mec1/ATR checkpoint kinase. *J.Biol.Chem*. 283(51):35853-9.

Navadgi-Patil, V.M., Burgers, P.M. (2009). The unstructured C-terminal tail of the 9-1-1 clamp subunit Ddc1 activates Mec1/ATR via two distinct mechanisms. *Mol.Cell*. 36(5):743-53.

Osborn, A.J., Elledge, S.J. (2003). Mrc1 is a replication fork component whose phosphorylation in response to DNA replication stress activates Rad53. *Genes.Dev.* 17(14):1755-67.

Paciotti, V., Lucchini, G., Plevani, P., Longhese, M.P. (1998). Mec1p is essential for phosphorylation of the yeast DNA damage checkpoint protein Ddc1p, which physically interacts with Mec3p. *EMBO.J.* 17(14):4199-209.

Pfander, B., Diffley, J.F.X. (2011). Dpb11 coordinates Mec1 kinase activation with cell cycle-regulated Rad9 recruitment. *EMBO J.* Epub 23 Sept. 2011.

Puddu F, Granata M, Di Nola L, Balestrini A, Piergiovanni G, Lazzaro F, Giannattasio M, Plevani P, Muzi-Falconi M. (2008). Phosphorylation of the budding yeast 9-1-1 complex is required for Dpb11 function in the full activation of the UV-induced DNA damage checkpoint. *Mol.Cell.Biol.* 28(15):4782-93.

Puddu, F., Piergiovanni, G., Plevani, P., Muzi-Falconi, M. (2011). Sensing of replication stress and Mec1 activation act through two independent pathways involving the 9-1-1 complex and DNA polymerase ϵ . *PLoS.Genet.* 7(3):e1002022.

Rouse, J., Jackson, S.P. (2002). Lcd1p recruits Mec1p to DNA lesions in vitro and in vivo. *Mol.Cell.* 9(4):857-69.

Saka, Y., Esashi, F., Matsusaka, T., Mochida, S., Yanagida, M. (1997). Damage and replication checkpoint control in fission yeast is ensured by interactions of Crb2, a protein with BRCT motif, with Cut5 and Chk1. *Genes Dev.* 11(24):3387-400.

Schwartz, M.F., Duong, J.K., Sun, Z., Morrow, J.S., Pradhan, D., Stern, D.F. (2002). Rad9 phosphorylation sites couple Rad53 to the *Saccharomyces cerevisiae* DNA damage checkpoint. *Mol.Cell.* 9(5):1055-65.

Segurado, M., Diffley, J.F. (2008). Separate roles for the DNA damage checkpoint protein kinases in stabilizing DNA replication forks. *Genes Dev.* 22(13):1816-27.

Shimada, K., Pasero, P., Gasser, S.M. (2002). ORC and the intra-S-phase checkpoint: a threshold regulates Rad53p activation in S phase. *Genes Dev.* 16(24):3236-52.

Sun, Z., Hsiao, J., Fay, D.S., Stern, D.F. (1998). Rad53 FHA domain associated with phosphorylated Rad9 in the DNA damage checkpoint. *Science.* 281(5374):272-4.

Sweeney FD, Yang F, Chi A, Shabanowitz J, Hunt DF, Durocher D. (2005). *Saccharomyces cerevisiae* Rad9 acts as a Mec1 adaptor to allow Rad53 activation. *Curr.Biol.* 15(15):1364-75.

Tercero JA, Longhese MP, Diffley JF. (2003). A central role for DNA replication forks in checkpoint activation and response. *Mol.Cell.* 11(5):1323-36.

Tourrière, H., Pasero, P. (2007). Maintenance of fork integrity at damaged DNA and natural pause sites. *DNA Repair(Amst).* 6(7):900-13.

Usui, T., Foster, S.S., Petrini, J.H. (2009). Maintenance of the DNA-damage checkpoint requires DNA-damage-induced mediator protein oligomerization. *Mol.Cell.* 33(2):147-59.

Vialard, J.E., Gilbert, C.S., Green, C.M., Lowndes, N.F. (1998). The budding yeast Rad9 checkpoint protein is subjected to Mec1/Tel1-dependent hyperphosphorylation and interacts with Rad53 after DNA damage. *EMBO J.* 17(19):5679-88.

Wang, H., Elledge, S.J. (1999). DRC1, DNA replication and checkpoint protein 1, functions with DPB11 to control DNA replication and the S-phase checkpoint in *Saccharomyces cerevisiae*. *Proc.Natl.Acad.Sci.USA.* 96(7):3824-9.

Wang H, Elledge SJ. (2002). Genetic and physical interactions between DPB11 and DDC1 in the yeast DNA damage response pathway. *Genetics.* 2002 Apr;160(4):1295-304.

Zou, L., Elledge, S.J. (2003). Sensing DNA damage through ATRIP recognition of RPA-ssDNA complexes. *Science.* 300(5625):1542-8.

Zou, L., Liu, D., Elledge, S.J. (2003). Replication protein A-mediated recruitment and activation of Rad17 complexes. *Proc.Natl.Acad.Sci.USA.* 100(24):13827-32.

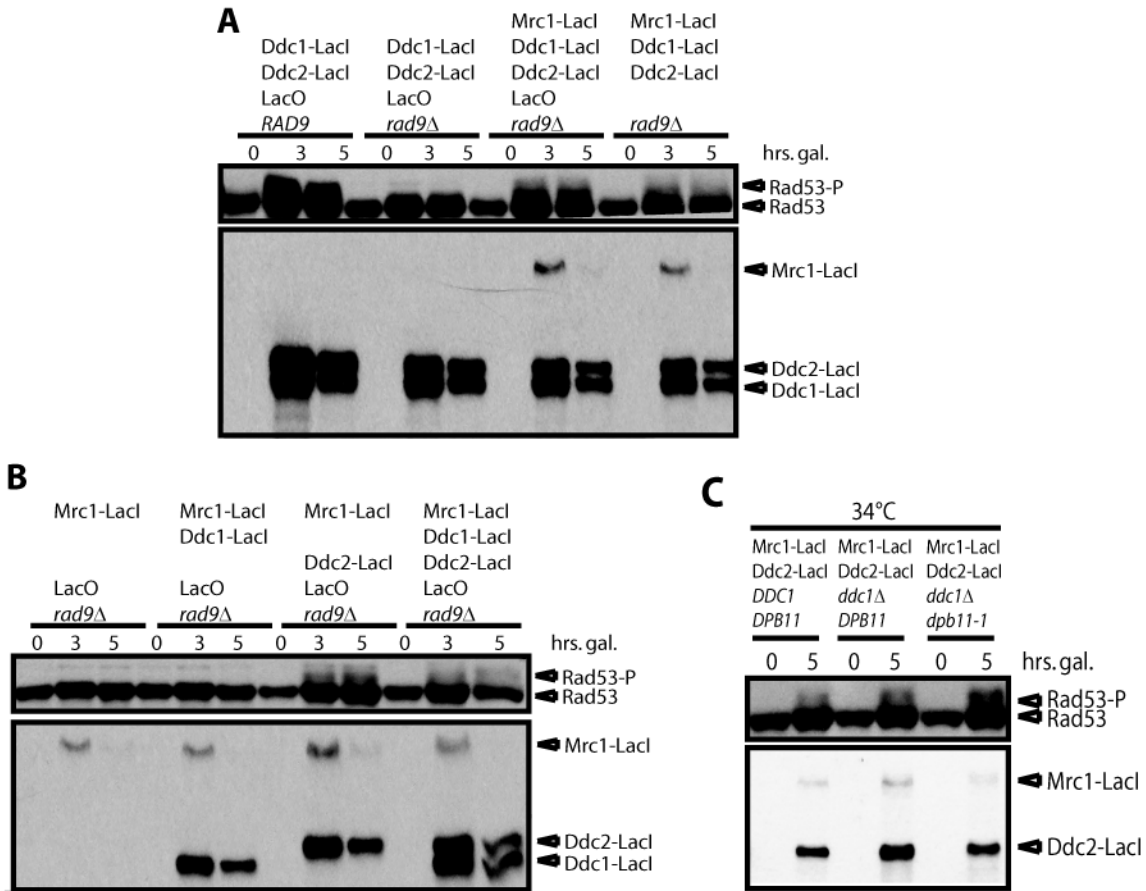


Figure 1. Co-localization of Mec1-Ddc2 and Mrc1 promotes Rad53 phosphorylation independent of Ddc1 and Dpb11. (A and B) Strains, with or without a LacO array and with the indicated combination of Mrc1-LacI, Ddc2-LacI, and Ddc1-LacI under the control of Gal promoter, were grown in raffinose and arrested in nocodazole for 3 hours. Galactose was pulsed for 1 hour before transcription was inhibited with dextrose, and then samples were collected at the indicated timepoints and blotted for Rad53 and the LacI fusion proteins. (C) As in A and B, except that strains were grown at 23°C, arrested with nocodazole, and either kept at 23°C or shifted to 34°C one hour before galactose induction.

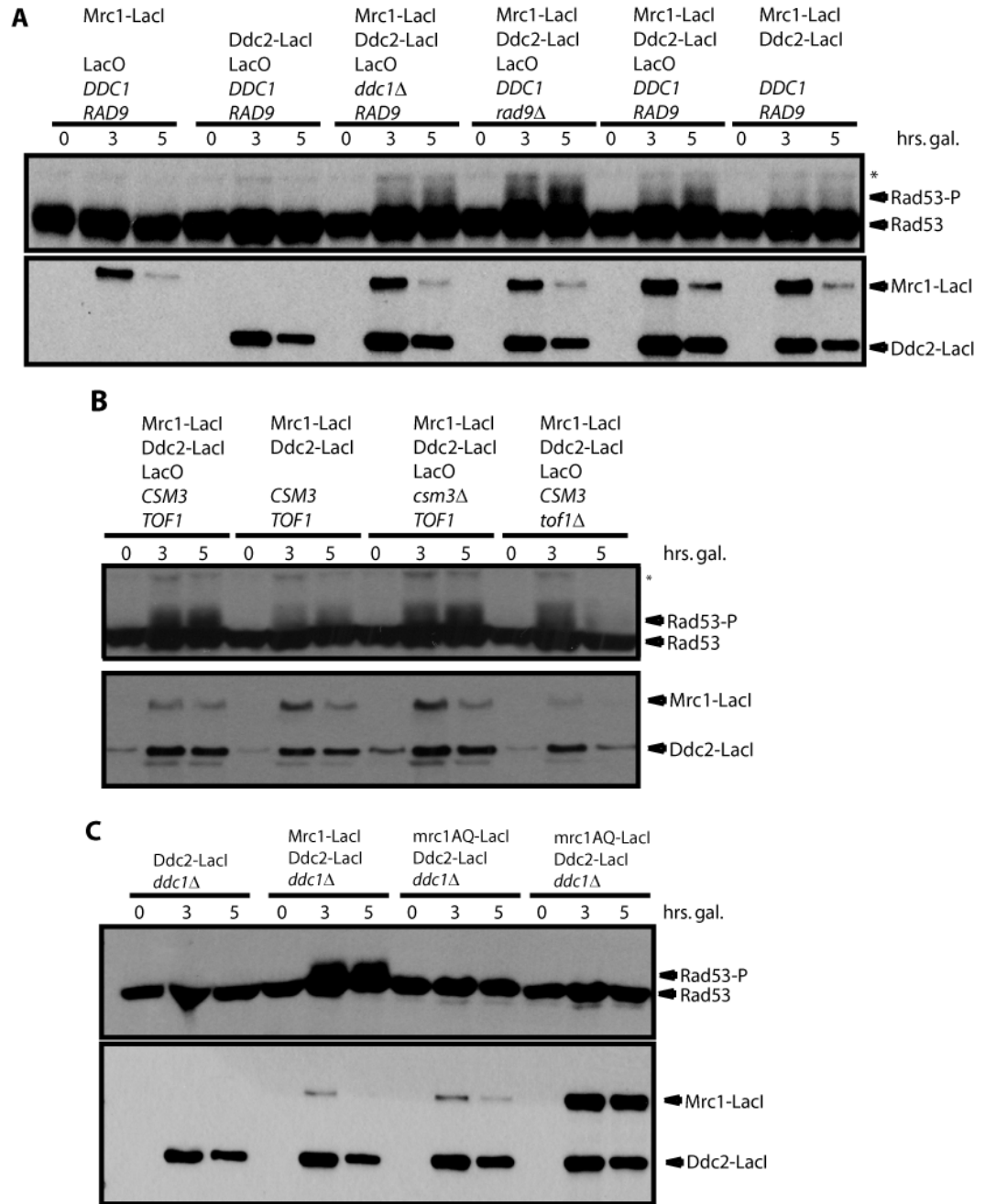


Figure 2. The replication-checkpoint mimic faithfully reproduces qualities of the replication checkpoint. (A) As in Figure 1, but Mrc1-LacI expression was increased so that it was similar to that of Ddc2-LacI. (B) The replication-checkpoint mimic was examined, as in A, in cells lacking the Mrc1 binding partners Csm3 or Tof1. (C) A *ddc1Δ* strain containing Ddc2-

LacI and LacO was transformed with either no additional fusion protein, Mrc1-LacI, *mrc1*^{AQ}-LacI, or high levels of *mrc1*^{AQ}-LacI and assayed as in A.

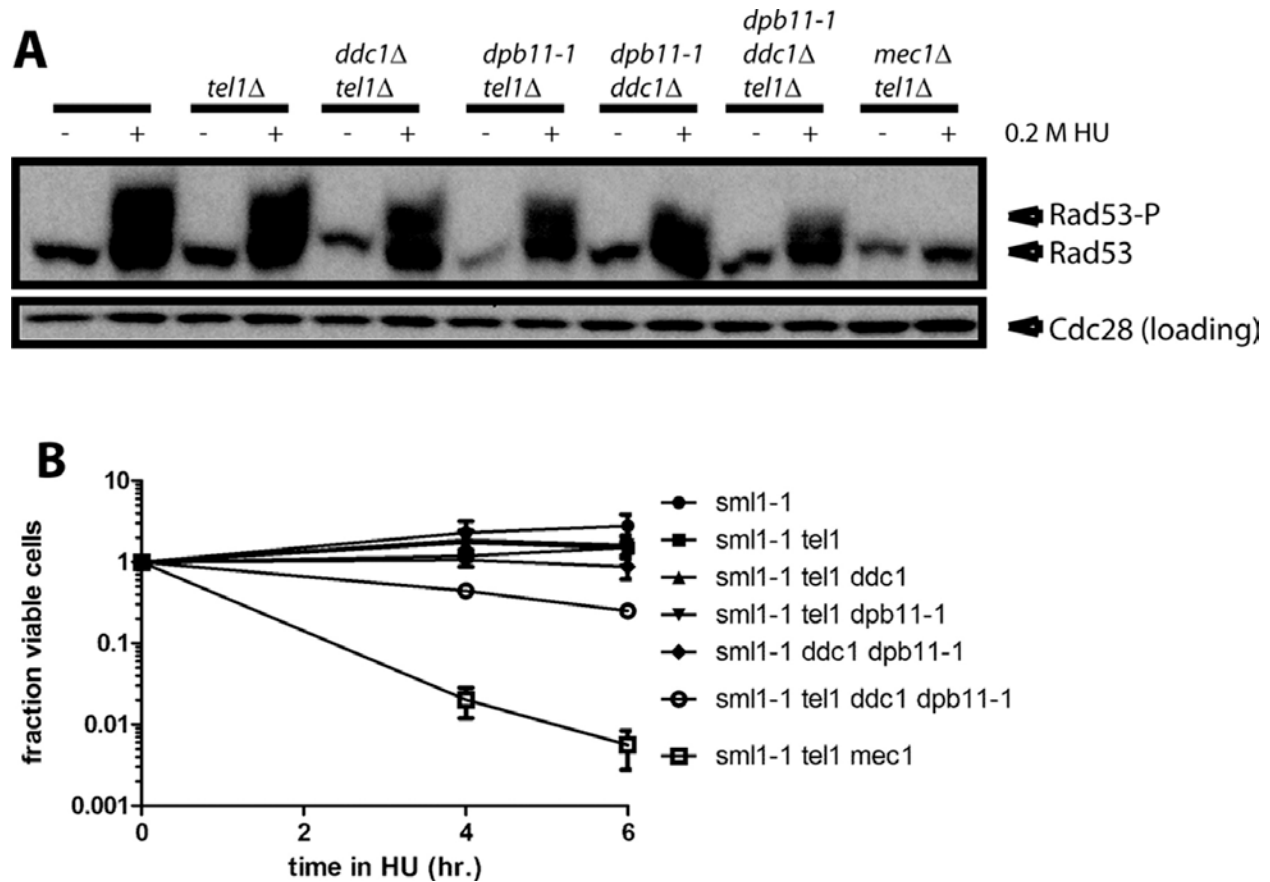


Figure 3. Rad53 can be phosphorylated in response to replication stress in the absence of 9-1-1 and Dpb11. (A) Strains with the indicated genotype were grown asynchronously and then treated with 0.2 M hydroxyurea (HU) for 4 hours at 22.5°C. All strains carry the *sml1-1* mutation, which suppresses lethality of a *mec1Δ*. Rad53 phosphorylation was visualized by SDS-PAGE and western blot. Cdc28 serves as a loading control. (B) After HU treatment as described in A for the indicated time, HU was washed out and cells plated on rich medium to determine viability. The mean of three independent experiments is plotted; error bars reflect standard error. (Error bars that cannot be seen are thinner than the line.)

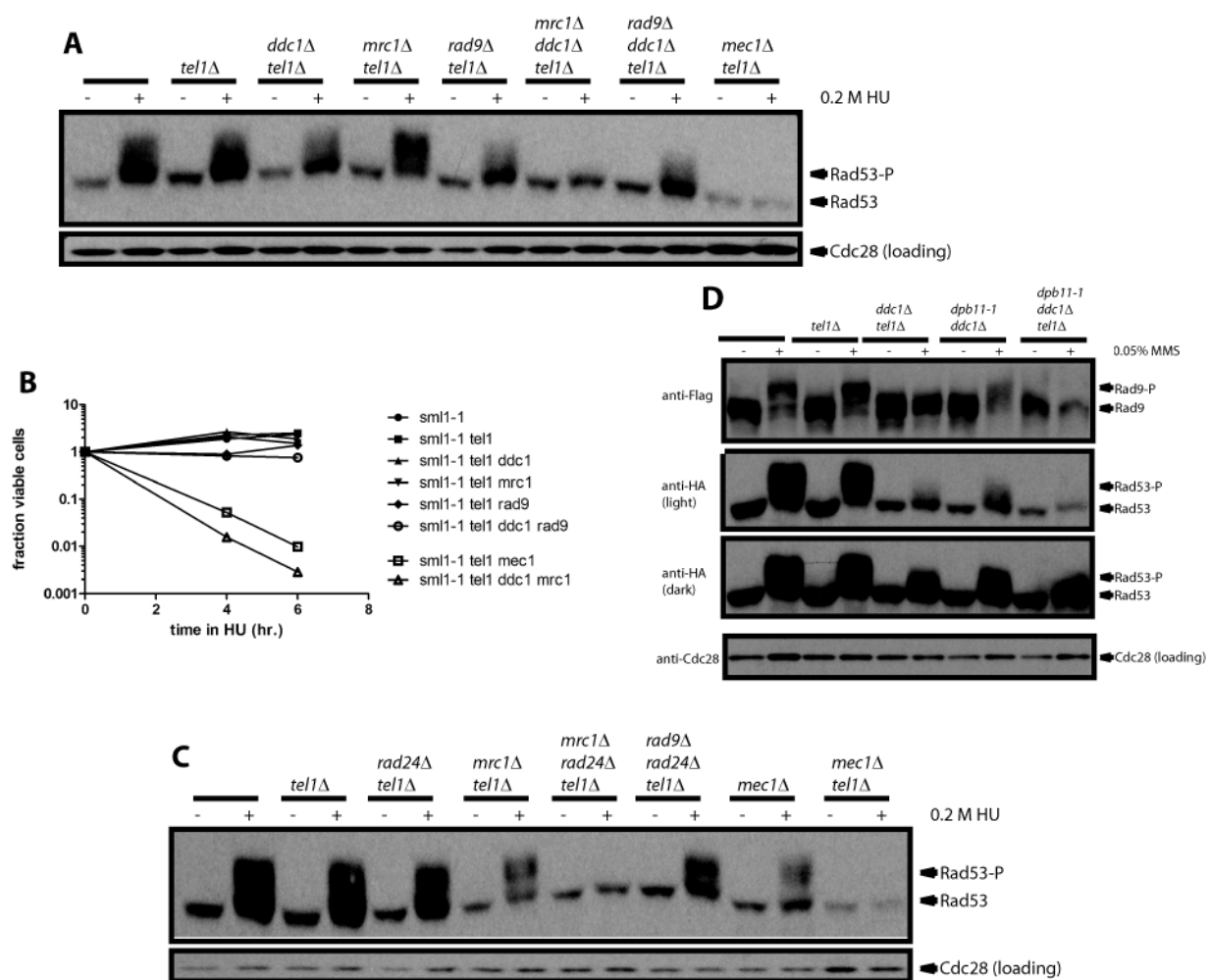


Figure 4. Rad53 phosphorylation in the absence of 9-1-1 requires Mrc1. (A) Cells of the indicated genotype were treated with HU for 2.5 hours at 30°C. All strains carry the *sml1-1* mutation, which suppresses lethality of *mec1Δ*. Rad53 phosphorylation was visualized by SDS-PAGE and western blot. Cdc28 served as a loading control. (B) After HU treatment as described in A for the indicated time, HU was washed out and cells were plated on rich medium to measure viability. (C) Cells of the indicated genotype were treated with HU for 2.8 hours at 30°C, and processed as in A. (D) Cells of the indicated genotype were treated with MMS for 4 hr. at 22.5°C, and phosphorylation of Flag-tagged Rad9 and Rad53-HA were visualized by SDS-PAGE and western blotting.

Table 1

Figure location	Strain name	Genotype	Source
1A, strain 1	CBY88	Mat a <i>ade2-1 Gal-Ddc2-Lacl::HIS3 Rad53-HA::LEU2 LacO₂₅₆::TRP1 GalS-Ddc1-Lacl::URA3 ddc1Δ</i>	Bonilla <i>et al.</i> , 2008
1A, strain 2	CBY90	Mat a <i>ade2-1 Gal-Ddc2-Lacl::HIS3 Rad53-HA::LEU2 LacO₂₅₆::TRP1 GalS-Ddc1-Lacl::URA3 ddc1Δ rad9Δ::hyg^R</i>	Bonilla <i>et al.</i> , 2008
1A, strain 3 1B, strain 4	TBY66	Mat a <i>GalS-Mrc1-Lacl::ADE2 Gal-Ddc2-Lacl::HIS3 Rad53-HA::LEU2 LacO₁₈₀::TRP1 GalS-Ddc1-Lacl::URA3 ddc1Δ rad9Δ::hyg^R</i>	This study
1A, strain 4	TBY63	Mat a <i>GalS-Mrc1-Lacl::ADE2 Gal-Ddc2-Lacl::HIS3 Rad53-HA::LEU2 trp1 GalS-Ddc1-Lacl::URA3 ddc1Δ rad9Δ::hyg^R</i>	This study
1B, strain 1	TBY60	Mat a <i>GalS-Mrc1-Lacl::ADE2 his3 Rad53-HA::LEU2 LacO₁₈₀::TRP1 ura3 ddc1Δ rad9Δ::hyg^R</i>	This study
1B, strain 2	TBY61	Mat a <i>GalS-Mrc1-Lacl::ADE2 his3 Rad53-HA::LEU2 LacO₁₈₀::TRP1 GalS-Ddc1-Lacl::URA3 ddc1Δ rad9Δ::hyg^R</i>	This study
1B, strain 3	TBY65	Mat a <i>GalS-Mrc1-Lacl::ADE2 Gal-Ddc2-Lacl::HIS3 Rad53-HA::LEU2 LacO₁₈₀::TRP1 ura3-1 ddc1Δ rad9Δ::hyg^R</i>	This study

1C, strain 1 and 4	TBY79	Mat a <i>GalS-Mrc1-Lacl::ADE2 Gal-Ddc2-Lacl::HIS3 Rad53-HA::LEU2 LacO₁₈₀::TRP1 ura3-1</i>	This study
1C, strain 2 and 5	TBY80	Mat a <i>GalS-Mrc1-Lacl::ADE2 Gal-Ddc2-Lacl::HIS3 Rad53-HA::LEU2 LacO₁₈₀::TRP1 ura3-1 ddc1Δ</i>	This study
1C, strain 3 and 6	TBY81	Mat a <i>GalS-Mrc1-Lacl::ADE2 Gal-Ddc2-Lacl::HIS3 Rad53-HA::LEU2 LacO₁₈₀::TRP1 ura3-1 ddc1Δ dpb11-1</i>	This study
2A, strain 1	TBY217	Mat a <i>Gal-Mrc1-Lacl::ADE2 his3-11,15 Rad53-HA::LEU2 LacO₂₅₆::TRP1 ura3-1</i>	This study
2A, strain 2 2C, strain 2	TBY206	Mat a <i>ade2 Gal-Ddc2-Lacl::HIS3 Rad53-HA::LEU2 LacO₂₅₆::TRP1 ura3-1</i>	This study
2A, strain 3	TBY34	Mat a <i>Gal-Mrc1-Lacl::ADE2 Gal-Ddc2-Lacl::HIS3 Rad53-HA::LEU2 LacO₂₅₆::TRP1 ura3-1 rad9Δ::hyg^R</i>	This study
2A, strain 4	TBY214	Mat a <i>Gal-Mrc1-Lacl::ADE2 Gal-Ddc2-Lacl::HIS3 Rad53-HA::LEU2 LacO₂₅₆::TRP1 ura3-1 ddc1Δ</i>	This study
2A, strain 5 2B, strain 1	TBY205	Mat a <i>Gal-Mrc1-Lacl::ADE2 Gal-Ddc2-Lacl::HIS3 Rad53-HA::LEU2 LacO₂₅₆::TRP1 ura3-1</i>	This study
2A, strain 6 2B, strain 2	TBY207	Mat a <i>Gal-Mrc1-Lacl::ADE2 Gal-Ddc2-Lacl::HIS3 Rad53-HA::LEU2 trp1-1 ura3-1</i>	This study
2B, strain 3	TBY36	Mat a <i>Gal-Mrc1-Lacl::ADE2 Gal-Ddc2-Lacl::HIS3 Rad53-HA::LEU2 LacO₂₅₆::TRP1 ura3-1 csm3Δ::g418^R</i>	This study

2B, strain 4	TBY38	Mat a <i>Gal-Mrc1-Lacl::ADE2 Gal-Ddc2-Lacl::HIS3 Rad53-HA::LEU2 LacO₂₅₆::TRP1 ura3-1 tof1Δ::g418^R</i>	This study
2C, strain 1	TBY236	Mat a <i>GalS-Mrc1-Lacl::ADE2 Gal-Ddc2-Lacl::HIS3 Rad53-HA::LEU2 LacO₂₅₆::TRP1 ura3-1</i>	This study
2C, strain 3	TBY238	Mat a <i>GalS-Mrc1AQ-Lacl::ADE2 Gal-Ddc2-Lacl::HIS3 Rad53-HA::LEU2 LacO₂₅₆::TRP1 ura3-1</i>	This study
2C, strain 4	TBY239	Mat a <i>GalS-Mrc1AQ-Lacl::ADE2 Gal-Ddc2-Lacl::HIS3 Rad53-HA::LEU2 LacO₂₅₆::TRP1 ura3-1</i>	This study
3AB, strain 1 4AB, strain 1 4C, strain 1	PGY182 4	Mat a <i>ade2-1 his3-11,15 leu2-3,112 lys2 RAD53-HA::TRP1 ura3-1 sml1-1</i>	Peter Garber, Toczyski lab
3AB, strain 2 4AB, strain 2 4C, strain 2	PGY252 5	Mat a <i>ade2-1 his3-11,15 leu2-3,112 lys2 RAD53-HA::TRP1 tel1Δ::URA3 sml1-1</i>	Peter Garber, Toczyski lab
3AB, strain 3	TBY326	Mat a <i>ade2-1 his3-11,15 leu2-3,112 lys2 RAD53-HA::TRP1 tel1::URA3 sml1-1 ddc1Δ::g418^R</i>	This study

4AB, strain 3			
3AB, strain 4	TBY380	Mat a <i>ade2-1 his3-11,15 leu2-3,112 lys2 RAD53-HA::TRP1 ura3-11,15 sml1-1 ddc1Δ::g418^R dpb11-1</i>	This study
3AB, strain 5	TBY327	Mat a <i>ade2-1 his3-11,15 leu2-3,112 lys2 RAD53-HA::TRP1 tel1::URA3 sml1-1 ddc1Δ::g418^R dpb11-1</i>	This study
3AB, strain 6 4AB, strain 8 4C, strain 8	TBY143	Mat a <i>ade2-1 his3-11,15 leu2-3,112 lys2 RAD53-HA::TRP1 mec1::TRP1 tel1::URA3 sml1-1</i>	This study
3B, strain 4	TBY233	Mat alpha <i>ade2-1 leu2-3,112 his4 RAD53-HA::TRP1 tel1::URA3 sml1-1 dpb11-1</i>	This study
4AB, strain 4	TBY51	Mat a <i>ade2-1 leu2-3,112 lys2 RAD53-HA::TRP1 tel1::URA3 sml1-1 mrc1Δ::nat^R</i>	This study
4AB, strain 5	TBY49	Mat a <i>ade2-1 leu2-3,112 lys2 RAD53-HA::TRP1 tel1::URA3 sml1-1 rad9Δ::hyg^R</i>	This study
4AB, strain 6	TBY50	Mat a <i>ade2-1 leu2-3,112 RAD53-HA::TRP1 tel1::URA3 sml1-1 ddc1Δ::g418^R mrc1Δ::nat^R</i>	This study
4AB, strain 7	TBY371	Mat a <i>ade2-1 leu2-3,112 RAD53-HA::TRP1 tel1::URA3 sml1-1 ddc1Δ::g418^R rad9Δ::hyg^R</i>	This study
4C, strain 4	PGY238 3	Mat a <i>ade2-1 his3-11,15 leu2-3,112 lys2 RAD53-HA::TRP1 tel1::URA3 sml1-1 mrc1::g418^R</i>	Peter Garber, Toczyski lab

4C, strain 5	PGY238 7	Mat a <i>ade2-1 his3-11,15 leu2-3,112 lys2 RAD53-HA::TRP1 rad24::TRP1 tel1::URA3 sml1-1 mrc1::g418^R</i>	Peter Garber, Toczyski lab
4C, strain 6	PGY221 5	Mat a <i>ade2-1 rad9::HIS3 leu2-3,112 lys2 RAD53-HA::TRP1 rad24::TRP1 tel1::URA3 sml1-1</i>	Peter Garber, Toczyski lab
4D, strain 1	TBY409	Mat a <i>ade2-1 his3-11,15 leu2-3,112 lys2 RAD53-HA::TRP1 ura3-1 sml1-1 RAD9-3xFLAG::hyg^R</i>	This study
4D, strain 2	TBY410	Mat a <i>ade2-1 his3-11,15 leu2-3,112 lys2 RAD53-HA::TRP1 tel1::URA3 sml1-1 RAD9-3xFLAG::hyg^R</i>	This study
4D, strain 3	TBY411	Mat a <i>ade2-1 his3-11,15 leu2-3,112 lys2 RAD53-HA::TRP1 tel1::URA3 sml1-1 RAD9-3xFLAG::hyg^R ddc1Δ::g418^R</i>	This study
4D, strain 4	TBY412	Mat a <i>ade2-1 his3-11,15 leu2-3 lys2 RAD53-HA::TRP1 sml1-1 RAD9-3xFLAG::hyg^R ddc1Δ::g418^R dpb11-1</i>	This study
4D, strain 5	TBY413	Mat a <i>ade2-1 his3-11,15 leu2-3,112 lys2 RAD53-HA::TRP1 tel1::URA3 sml1-1 RAD9-3xFLAG::hyg^R ddc1Δ::g418^R dpb11-1</i>	This study
S1, strain 1	ADR21	Mat a <i>ade2-1 can1-100 his3-11,15 leu2-3,112 trp1-1 ura3-1</i>	Adam Rudner, A. Murray lab
S1, strain 2		Mat a <i>ade2-1 his3-11,15 leu2-3,112 trp1-1 ura3-1 dpb11-1</i>	Gift of H. Araki

Supplemental Material for “Co-localization of Mec1 and Mrc1 is sufficient for Rad53 phosphorylation *in vivo*”

Supplemental Methods

Rad53 in situ kinase assay (ISA)

ISAs were performed according to the protocol of Pellicoli *et al.* (1999). Cell pellets were TCA-precipitated, run on an SDS-PAGE gel, and transferred to a PVDF membrane in buffer containing methanol. Membranes were rinsed briefly with TBST, denatured for one hour at room temperature in 7M guanidine-HCL/50 mM dithiothreitol (DTT)/2 mM EDTA/50 mM Tris-HCl pH 8.0, washed twice with 1X TBS, and then renatured overnight at 4°C with four changes of buffer in 2 mM DTT/2 mM EDTA/0.04% Tween-20/10mM Tris-HCl pH 7.5/140 mM NaCl/1% BSA. Membranes were then incubated at room temperature for 1 hour in 30 mM Tris-HCl, pH 7.5 before pre-equilibration in kinase buffer (1mM DTT, 0.1 mM EGTA, 20 mM MgCl₂, 20 mM MnCl₂, 40 mM Hepes-NaOH pH 8.0, 0.1 mM sodium orthovanadate) for 30 minutes at room temperature. Kinase assays were then performed in fresh kinase buffer in the presence of 100μCi per membrane [γ -³²P]ATP for one hour at room temperature. Membranes were washed for 10 minutes each in 30 mM Tris-HCl pH 7.5, 30 mM Tris-HCl pH 7.5, 30 mM Tris-HCl pH 7.5/0.1% NP-40, 30 mM Tris-HCl pH 7.5, 1M KOH, water, 10% TCA, and water, and then dried and exposed to a PhosphorImager.

Rad53 activation was quantified by measuring the intensity of the Rad53 band and of the background band that serves as a loading control, and subtracting the background of the blank membrane from each. Then, the corrected intensity of the Rad53 band was divided by the corrected intensity of the loading control to give the relative Rad53 intensity. The highest

intensity was set to 1. To give the Rad53 activation for each strain, the relative Rad53 intensity of the untreated sample was subtracted from the relative Rad53 intensity of the HU- or MMS-treated sample.

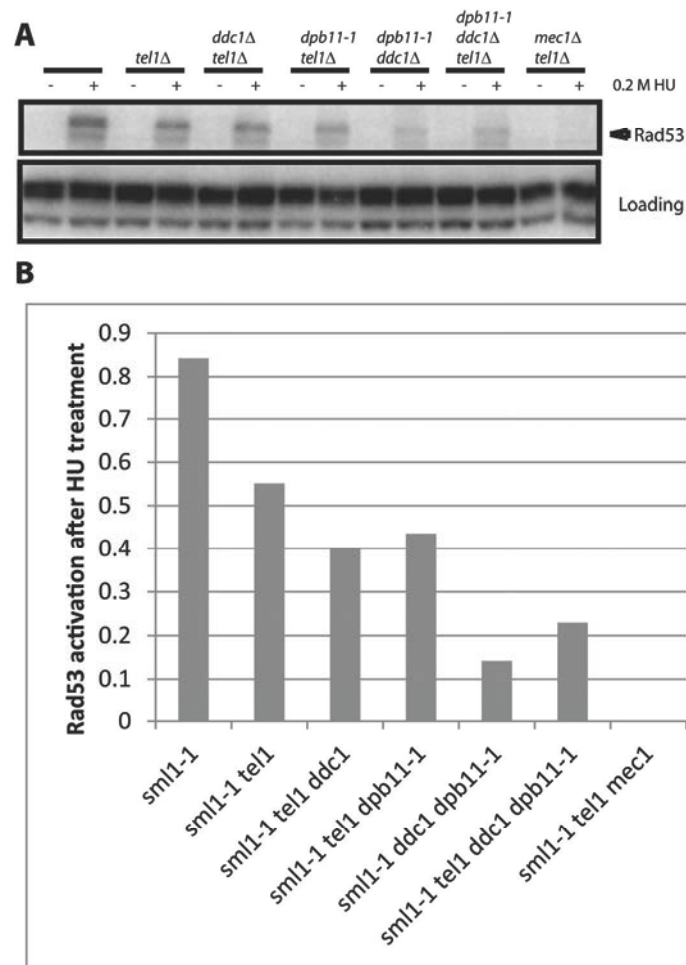
Supplemental References

Pelliccioli, A., Lucca, C., Liberi, G., Marini, F., Lopes, M., Plevani, P., Romano, A., Di Fiore, P.P., Foiani, M. (1999). Activation of Rad53 kinase in response to DNA damage and its effect in modulating phosphorylation of the lagging strand DNA polymerase. *EMBO J.* 18(22): 6581-72.

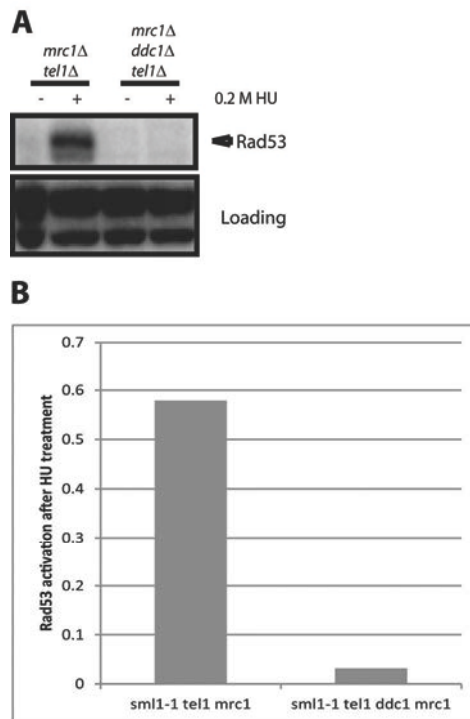
Figure Legends



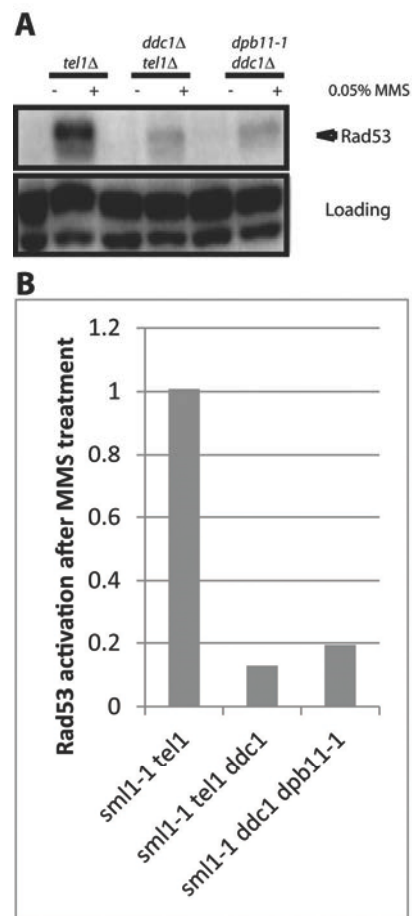
Supplementary Figure S1. *dpb11-1* cells cannot grow at 34°C



Supplementary Figure S2 (related to Figure 3). Rad53 can be activated in response to replication stress in the absence of 9-1-1 and Dpb11. (A) Strains with the indicated genotype were grown asynchronously and then treated with 0.2 M hydroxyurea (HU) for 4 hours at 22.5°C. All strains carry the *sml1-1* mutation, which suppresses lethality of a *mec1Δ*. Rad53 activation was assayed by ISA. (B) Rad53 activation was quantified as described in the Supplemental Methods.



Supplementary Figure S3 (related to Figure 4A). Rad53 phosphorylation in the absence of 9-1-1 requires Mrc1. (A) Strains with the indicated genotype were grown asynchronously and then treated with 0.2 M HU for 4 hours at 22.5°C. All strains carry the *sml1-1* mutation, which suppresses lethality of a *mec1Δ*. Rad53 activation was assayed by ISA. (B) Rad53 activation was quantified as described in the Supplemental Methods.



Supplementary Figure S4 (related to Figure 4D). Rad53 activation in response to MMS is equivalent in *ddc1Δ tel1Δ* and *ddc1Δ dpb11-1* mutants. (A) Strains with the indicated genotype were grown asynchronously and then treated with 0.05% methyl methanesulfonate (MMS) for 4 hours at 22.5°C. All strains carry the *sml1-1* mutation, which suppresses lethality of a *mec1Δ*. Rad53 activation was assayed by ISA. (B) Rad53 activation was quantified as described in the Supplemental Methods.

Chapter 3:

DNA damage regulates translation through β -TRCP targeting of CReP

Theresa B. Loveless¹, Benjamin R. Topacio¹, Ajay A. Vashisht², Shastyn Galaang¹, Katie M. Ulrich¹, Brian D. Young², James A. Wohlschlegel², and David P. Toczyski^{1,3}

¹Department of Biochemistry and Biophysics

Helen Diller Family Comprehensive Cancer Center

University of California, San Francisco

²Department of Biological Chemistry

University of California, Los Angeles

³To whom correspondence should be addressed: toczyski@cc.ucsf.edu

Running Head: DNA damage regulates translation through β -TRCP targeting of CReP

Keywords: DNA damage; genome instability; ubiquitin ligase; Ligase Trapping; translation

Abstract

The Skp1-Cul1-F box complex (SCF) associates with any one of a number of F box proteins, which serve as substrate binding adaptors. The human F box protein β TRCP directs the conjugation of ubiquitin to a variety of substrate proteins, leading to the destruction of the substrate by the proteasome. To identify β TRCP substrates, we employed a recently-developed technique, called Ligase Trapping, wherein a ubiquitin ligase is fused to a ubiquitin-binding domain to “trap” ubiquitinated substrates. 88% of the candidate substrates that we examined were bona fide substrates, comprising twelve previously validated substrates, eleven new substrates and three false positives. One β TRCP substrate, CReP, is a Protein Phosphatase 1 (PP1) specificity subunit that targets the translation initiation factor eIF2 α to promote the removal of a stress-induced inhibitory phosphorylation and increase cap-dependent translation. We found that CReP is targeted by β TRCP for degradation upon DNA damage. Using a stable CReP allele, we show that depletion of CReP is required for the full induction of eIF2 α phosphorylation upon DNA damage, and contributes to keeping the levels of translation low as cells recover from DNA damage.

Author Summary

Approximately 600 human genes encode enzymes that act as ubiquitin ligases, which facilitate the transfer of the small protein ubiquitin to thousands of substrate proteins; “tagging” with ubiquitin often promotes the degradation of the substrate by the proteasome. In this paper, we adapt a technique called Ligase Trapping for use in mammalian cells. Ligase Trapping is a highly accurate method for determining which substrates are targeted by a ubiquitin ligase. Here we use it to identify new substrates of the human cell cycle regulator β TRCP. Our screen was indeed highly accurate, as we were able to validate 88% of the candidate substrates we identified by mass spectrometry. Some of these new substrates were unstable proteins that were stabilized by inhibition of β TRCP, or of the entire class of ubiquitin ligases of which β TRCP

is a part. However, others appear to be stable or redundantly-targeted substrates, which have been more difficult to identify with current techniques. This suggests that Ligase Trapping will be able to reliably identify new substrates of human ubiquitin ligases. Further, one of the new β TRCP substrates, CReP, is specifically depleted upon DNA damage, and depletion of CReP contributes to inactivation of the translational machinery upon DNA damage.

Introduction

E3 ubiquitin ligases, which facilitate the attachment of anywhere from one to a long chain of the small protein ubiquitin to substrate proteins, are important regulators of the cell cycle and the response to stress. The best-studied outcome of ubiquitination is destruction of the substrate by the proteasome. There has been a great deal of interest in the discovery of ubiquitin ligase substrates, with the recent introduction of techniques that either look for proteins whose levels change when a particular ubiquitin ligase is inhibited [1-5], or those that use mass spectrometry to look for proteins that interact physically with the ubiquitin ligase [6-11]. Unfortunately, some ligase-substrate interactions are likely too weak to purify by affinity. Moreover, once a list of associated proteins is identified, it is not always clear which are direct substrates. To address this, most studies have determined whether the half-life of the substrate is significantly altered upon inhibition of the ligase [11]. However, in many instances, only a select fraction of substrate is targeted. In addition, some substrates are targeted redundantly by multiple ligases [12]. These facts often make it impossible to verify candidates merely by examining their half-life. For ubiquitin ligases for which a consensus binding sequence is known, the presence of this sequence has been used frequently to separate true substrates from non-substrate or non-specific interactors. However, this method is not useful to discover substrates of the vast majority of ubiquitin ligases, for which no consensus sequence is known. To eliminate these problems, we developed a technique called Ligase Trapping [13] (Fig 1A), in which an E3 ubiquitin ligase is fused to a ubiquitin-associated (UBA) domain. This mediates an

extended interaction between the E3 ligase and its ubiquitinated substrates, allowing their co-immunoprecipitation. To distinguish between substrates and other associated proteins, this immunoprecipitate is subjected to a second purification for 6xHIS-ubiquitin under denaturing conditions. These purifications can be used both for substrate identification and as a diagnostic for candidate confirmation, in cases where the bulk level of a protein is stable.

The SCF is a cullin-RING ligase (CRL) containing 3 core catalytic subunits: the RING finger protein RBX1, the cullin CUL1 and the adaptor SKP1 [14-17]. This catalytic base associates with a substrate adaptor called an F box protein, of which humans encode at least 69. F box proteins are thought to recognize their substrates only after substrate modification, typically by phosphorylation [14,17]. Several of these F box proteins have been characterized due to their well-established roles as tumor suppressors and oncogenes. β TRCP[18] is an F box protein that turns over substrates to control the G2/M transition (*e.g.* WEE1 [19]/CDC25 [20,21]), as well as the response to DNA damage (*e.g.* CDC25 [20,21], claspin [7,22]).

In this paper, we establish ubiquitin ligase trapping in mammalian cells. Of the 28 candidates identified using this technique, 12 were well-established substrates [6,20,21,23-33]. For the 16 remaining candidates, we examined 14 and found that 11 of these confirmed. Thus, 23 of the 26 known/tested candidates (88%) appear to be substrates, suggesting that Ligase Trapping is a robust discovery technique. Further characterization showed that turnover of one of the β TRCP substrates, CReP, is exacerbated by DNA damage. CReP is a protein phosphatase 1 (PP1) specificity subunit that counteracts the phosphorylation of eukaryotic initiation factor 2 alpha (eIF2 α) on serine-51 [34], a stress-induced modification that inhibits translation initiation on most transcripts [35,36]. Inhibiting the turnover of CReP after DNA damage significantly reduced the accumulation of serine-51 phosphorylated eIF2 α , and increased translation after DNA damage, suggesting that CReP turnover is an important mechanism by which DNA damage regulates translation.

Results

To establish Ligase Trapping in human cells, we created a stable HEK293 line in which 6xHIS-ubiquitin is expressed upon treatment with doxycycline. In this cell line, tagged ubiquitin accounts for a significant portion of the total ubiquitin pool when cells are treated with doxycycline (S1A Fig). In yeast, fusion of F box proteins, via a 3xFlag linker, to the UBA of Dsk2 or the two tandem UBAs of Rad23, led to enhanced purification of nascent ubiquitinated F box protein substrates [13]. We fused the human F box protein β TRCP to the human homologs of these UBA-containing proteins, and found that the RAD23B fusion increased the poly-ubiquitinated species purified by the β TRCP fusion most strongly (S1B Fig). Accordingly, we made a stable cell line that expressed both doxycycline-inducible 6xHIS-Ub and a Ligase Trap consisting of β TRCP fused on its C-terminus to 3xFlag and the C-terminal UBAs of RAD23B.

To determine whether the β TRCP trap was functional, we expressed an epitope-tagged allele of the β TRCP substrate ATF4 in our stable cell line. We were able to immunoprecipitate poly-ubiquitinated ATF4 with the β TRCP trap, but not with the Ligase Traps of two unrelated F box proteins, FBXO24 and Fbw7 (Fig 1B). We obtained a similar result with β -catenin (S2 Fig). We also purified ubiquitinated forms of the Ligase Traps, which was unsurprising as many ubiquitin ligases are themselves ubiquitinated. We also purified substantial unmodified forms of the Ligase Traps. This is likely a result of the very large amount of IP loaded relative to input (5,000:1 for the 2nd step), which is necessary to see the very small percentage of substrate that is poly-ubiquitinated. Even in cases where the unmodified band is equal in intensity in the input and 2nd step IP, this represents only 0.02% IP background. This phenomenon also occurs frequently with unmodified substrates, while the relevant purification of poly-ubiquitinated substrates is highly specific to the relevant Ligase Trap. To examine further whether the purification of β -catenin was specific, we made a stable cell line identical to our β TRCP ligase trap line, but with a mutation in the WD40 domain of β TRCP predicted to prevent binding to β -

catenin[37]. As expected, this mutant trap failed to purify polyubiquitinated β -catenin (Fig 1C), showing that β -catenin purification by β TRCP represents a specific interaction. To make certain that the β TRCP Ligase Trap didn't simply bind all ubiquitinated proteins more efficiently, we made a similar stable cell line expressing Fbw7-3xFlag-RAD23. Poly-ubiquitinated forms of the known Fbw7 substrate MED13 [10] were preferentially precipitated with the Fbw7 Ligase Trap (Fig 1D).

Candidate Substrate	Locus ID	TSC 1	TSC 2	TSC 3	Ubiquitinated forms precipitated?	Stabilized by beta-TRCP knock down?	Stabilized by MLN4924?	beta-TRCP consensus binding motif
HIVEP1/2	P15822/ P31629	13	0	69	yes		*	DSGESEEE
Nrf2	Q16236	18	8	9				
CRP	Q5SWA1	12	11	13	yes	partial	yes	DDGFSD
UBE4B	O95155	17	5	23	yes	stable	stable	DTTFLLD
ATF-4	P18848	11	9	19				
CDC25A	P30304	11	7	14				
ZNF395	Q9H8N7	9	6	11	yes		yes	DSGSSTTS
ZNF704	Q6ZNC4	7	3	9	yes	partial	partial	DDGIDEAE/ SDGEED
PDCD4	Q53EL6	5	4	4				

bHLHE40	O14503	5	2	14	yes		*	
CDC25B	P30305	3	2	10				
BAT2	P48634	2	3	6	no			DSGGSSE/ DSGVDLS/D SGHCVPE
Deptor	Q8TB45	3	2	7				
SUN2	Q9UH99	3	3	0	yes		yes	DDGSSSS
AEBP2	Q6ZN18	1	2	6	yes	partial	partial	SDGEPLS
RAPGEF2	Q9Y4G8	3	0	5				
GGNP2	Q9H3C7	2	1	3				DSGKGAKS
TFAP4	Q01664	3	0	3	yes		yes	
Emi1	Q9UKT4	1	2	0				
Per2	O15055	2	0	3				
ALDH2	P05091	1	0	6	no			DGDFFSYT
WWTR1	Q9GZV5	2	0	2				
TRIM9	Q9C026	1	1	2	yes		*	DSGYGS
CEP44	Q9C0F1	1	1	0	no			SSGKSE
DACT1	Q9NYF0	1	1	0				SSGFYELS
FNIP1	Q8TF40	1	1	0	yes		no	DSGIARS
RIPK4	P57078	1	0	3	yes			DSGAS
RASSF3	Q86WH2	0	1	2	yes	no	no	SSGYSS
<i>NFκB</i> <i>p100</i>	Q00653	1	0	11				
<i>β-catenin</i>	P35222	33	18	36				

<i>eEF2K</i>	O00418	0	0	6				
<i>REST</i>	Q13127	0	0	12				

Table 1. Discovery and validation summary for identified β TRCP substrates. List of all proteins purified uniquely and at least twice by the β TRCP Ligase Trap, with total spectral counts (TSC) for each of three purifications. Two unique HLA alleles were excluded, as other HLA alleles were identified in negative control purifications. Substrates in normal text were previously well-described, and those in bold are novel, although some have previously been isolated in large-scale experiments. The substrates in italics are known β TRCP substrates that were isolated, but did not meet our criteria for candidates. For the validation experiments, a blank box means the experiment was not performed. * indicates that the protein appears stable even in the absence of the cullin inhibitor MLN4924. The closest to consensus β TRCP degron found in the primary sequence of each novel candidate is shown.

Having established the functionality of the β TRCP ligase trap cell line, we performed a large-scale, two-step purification and identified ubiquitinated co-precipitating proteins by mass spectrometry. Before collection, we treated cells with the proteasome inhibitor MG132 for four hours, as we had shown that this treatment increases the amount of poly-ubiquitinated material purified by the β TRCP ligase trap (S1C Fig). We defined candidate β TRCP substrates as those proteins identified in at least two of three purifications of the β TRCP ligase trap, but not in any of the negative control purifications. Twenty-eight proteins met these criteria (Table 1). Of these, twelve were previously-validated β TRCP substrates, and many others had been shown to interact with β TRCP in previously published large data sets, but had not been individually examined to determine if they were substrates [4,8,11,38-40]. SUN2 was purified in a large-scale screen for β TRCP substrates, and shown to be stabilized by the proteasome inhibitor MG132 [39] while this manuscript was under review. In addition, several other known β TRCP

substrates, such as β -catenin [41-45], were selectively identified in the β TRCP purification, but as some peptides were also identified in control purifications, these did not meet the stringent criteria that we had chosen for this initial analysis (bottom of Table 1). The large fraction of previously-published substrates (43%) that we purified confirms that Ligase Trapping accurately identified true substrates.

We also purified substrates of Fbw7 using a Ligase Trap. The Fbw7 Ligase Trap was expressed at a low level, suggesting that this trap was less stable. However, the proteins pulled down most abundantly and specifically by the Fbw7 Ligase Trap were MED13 and MED13L, two members of the Mediator complex shown to be Fbw7 substrates in a recent screen[10] in which Fbw7 interactors were precipitated and identified by mass spectrometry. (Our purification of MED13 is shown in Fig 1D.) In that screen, The entire 26-member Mediator complex was purified, and MED13 and MED13L had to be identified as the direct Fbw7 substrates by a combination of degron prediction and careful validation; we did not purify any other members of the Mediator complex.

Ligase Trapping also provided a method to validate candidates beyond simply examining substrate turnover. Ligase Trapping is able to show that a ubiquitinated substrate specifically purifies with a particular ligase even if the substrate is redundantly targeted by multiple ligases, or if only a small fraction of the substrate (such as that in a particular complex) is ubiquitinated. To fully assay the accuracy of the Ligase Trap technique, we decided to validate candidate β TRCP substrates. Out of fourteen of the previously unknown/unvalidated candidates that we examined, eleven showed specific purification of polyubiquitinated material by the β TRCP ligase trap (Table 1, Fig 2, and S4 Fig and S5 Fig). This strongly suggested that these candidates are true substrates of β TRCP, and that this technique accurately identified substrates with low background and thus will be an efficient way of identifying and validating

substrates of other ubiquitin ligases in the future. Two β TRCP candidate substrates were not examined due to technical difficulties.

In order to determine whether β TRCP could bind its candidate substrates in the absence of the UBA domains present in the Ligase Traps, we co-expressed Flag-tagged versions of these F box proteins in HEK293 cells with HA-tagged versions of a subset of their candidate substrates. In all cases, the substrate was purified more efficiently by its cognate ligase than by the negative control ligase (Fig 3A).

Because a common outcome of ubiquitination by the SCF is proteasomal degradation of the ubiquitinated protein, we assayed whether a subset of the candidate substrates were degraded in a way that depended on the cognate ligase. For five of the β TRCP candidate substrates, we co-transfected cells with DNA encoding tagged substrate, as well as a negative control plasmid or a plasmid expressing an shRNA targeting both paralogs of β TRCP, then inhibiting bulk protein translation with cycloheximide and assaying substrate levels. Although the knockdown we achieved was quite modest, three of the five substrates were significantly stabilized (Fig 3B). One, RASSF3, was not stabilized, suggesting either that it is a better β TRCP substrate than the others, or that it is targeted by other ubiquitin ligases. UBE4B is a stable protein. (Note that we detected UBE4B with a specific antibody against this protein, and did not ectopically express it, so its stability is unlikely to be an artifact.) It is possible that either only a small pool of the substrate was targeted, or that the outcome of ubiquitination of UBE4B is not proteasomal degradation.

Several commonly-used approaches identify ubiquitin ligase substrates as those proteins whose abundance is increased by inhibition of the relevant ligase. One key advantage of ligase trapping is that, in contrast to these techniques, it can identify substrates whose bulk turnover is not affected by inhibition of the ligase. To determine more universally which substrates were quantitatively targeted for degradation by β TRCP, we expressed tagged

versions of the substrates, inhibited protein synthesis with cycloheximide, and followed the turnover of the substrate in the absence or presence of MLN4924 (Table 1 and S6 Fig). Of the ten substrates examined, three (CReP, ZNF395, and SUN2) were unstable proteins that were stabilized by MLN4924, suggesting that their turnover is mediated by β TRCP alone or in combination with other cullin-RING ligases. (CReP was previously shown to be an unstable protein[34], as was SUN2.) Four (ZNF704, FNIP, RASSF3 and AEBP2) were not or only partially stabilized by MLN4924, suggesting that these might be redundantly targeted by β TRCP and a non-CRL ligase. Three proteins (HIVEP2, UBE4B, and TRIM9) appeared to be constitutively stable, although we cannot rule out that overexpression or epitope tagging of HIVEP2 and TRIM9 led to an artifactual stabilization. β TRCP could be promoting non-degradative ubiquitination of these substrates, or may only ubiquitinate a specific pool.

We were initially concerned that treating cells with MG132 would lead to increased background, or skewing of the results. Therefore, we performed two purifications of the β TRCP ligase trap in the absence of MG132. This purification generated a list with several of the same substrates, but lacking a subset, especially those shown to be unstable in Figures 3B and S6 (S7 Fig). In addition, all of our validations were performed in the absence of MG132 (Fig 2, S4 Fig, and S5 Fig).

We wished to further explore the biological significance of CReP turnover. First, we verified that the ubiquitinated CReP pulled down by the β TRCP ligase trap required SCF activity. Indeed, pre-treatment of cells with MLN4924 eliminated the ubiquitinated CReP (but not unmodified CReP) pulled down by the β TRCP ligase trap (Fig 4A). Second, we mutated CReP's single well-conserved β TRCP-binding consensus, as well as the amino acids immediately downstream, which form a second less-well-conserved consensus. The β TRCP consensus is DpSGX(1-4)pS[46], with some substitution of acidic amino acids for phosphorylations tolerated. The sequence we mutated in CReP is DDGFSDSSSLSDSD (marked in S11 Fig). Although this

sequence lacks the most-conserved DSG motif, many well-documented β TRCP substrates have variations in this part of the degron [18], and human CDC25A and CDC25B have well-validated degrons that contain DDG, just like CReP [25] (shown in Fig 4B). This mutant, CReP^{11A}, was significantly stabilized relative to wild type CReP (Fig 4C and Fig 4D), strongly suggesting that CReP turnover is dependent on β TRCP. The notable downshift of the mutant is likely due to mutation of several negatively-charged residues. Mutation of a portion of the same region was independently shown to stabilize CReP while our manuscript was in the review process[47].

Because both protein-folding stress and DNA damage have been shown to regulate eIF2 α phosphorylation, we tested whether these stresses also regulated CReP levels. The proteostatic stress inducer thapsigargin had a very minor effect on CReP levels, consistent with a previous report showing no effect [34]. However, DNA damage provoked by either ultraviolet light (UV) or the topoisomerase inhibitor camptothecin (CPT) led to complete depletion of CReP (Fig 5A). Suggestively, the disappearance of CReP was coincident with the induction of eIF2 α phosphorylation by these stressors. The depletion of CReP was not due merely to inhibition of translation by eIF2 α phosphorylation, as DNA damage also decreases the half-life of CReP compared to no treatment or treatment with proteostatic stressors in a cycloheximide chase (S11 Fig), and CReP still disappears upon DNA damage in mouse embryonic fibroblasts in which Ser51 of eIF2 α has been mutated to alanine (data not shown). CReP turnover and subsequent eIF2 α phosphorylation is at least partially dependent on β TRCP, as transfection with shRNA against both paralogs of this ligase delays DNA damage-dependent induction of both CReP turnover and eIF2 α phosphorylation (Fig 5B). CReP depletion is fully dependent on CRL-mediated degradation, because treatment of cells with the CRL inhibitor MLN4924 prevents CReP depletion (Fig 5C). The residual CReP turnover seen even in cells treated with β TRCP shRNA may reflect our inability to achieve sufficient knockdown of β TRCP, or additional

turnover mediated by another CRL. Cullin-mediated turnover of CReP in response to DNA damage was not restricted to HEK293 cells, since it occurs in both primary human fibroblasts (Fig 5D) and immortalized mouse embryonic fibroblasts (MEFs) (S12 Fig).

The CReP^{11A} mutant was not completely stabilized upon DNA damage (data not shown), possibly because DNA damage promotes β TRCP binding to additional sites on CReP. Therefore, we mapped phosphorylated residues on CReP to identify any additional degron sequences (S9 Fig). Notably, most phosphosites were observed both with and without CPT. It is possible that the increase in CReP turnover observed upon DNA damage is not due to increased phosphorylation, but to a change in a targeting factor or localization of CReP. However, phosphosites are still likely to be required for turnover. For clustered phosphosites and phosphosites that were near short acidic stretches, we mutated both the phospho-acceptor and all acidic and potential phospho-acceptors in the region. In addition, we mutated one additional weak β TRCP consensus site that was not covered in the phospho-mapping. We then tested the stability of these mutants, in various combinations, in DNA damage (data not shown). CReP^{31A} (S10 Fig) was the least mutated allele that was completely stable upon treatment with DNA damage (Fig 5E and Fig 5F). Importantly, this stabilization was not merely an artifact of high starting levels resulting from prioritized transcription or translation, as CReP^{31A} is stable even upon pre-treatment with camptothecin followed by cycloheximide chase (Fig 5E). Like the 11A mutant, CReP^{31A} migrates much more quickly than the endogenous protein, likely due to mutation of many negatively-charged amino acids.

To examine the physiologic role of the turnover of CReP upon DNA damage, we determined whether CReP stabilization had an effect on eIF2 α phosphorylation. When CReP turnover was inhibited by knockdown of β TRCP, treatment with MLN4924, or mutation of CReP, phosphorylation of eIF2 α was delayed or inhibited to an equivalent degree (Figs 5B, 5C, and 5F). This is not specific to HEK293 cells, as MLN4924 also reduced eIF2 α phosphorylation after

UV treatment in immortalized mouse embryonic fibroblasts (MEFs) (S12 Fig). However, primary human fibroblasts (Fig 6D) had constitutively high levels of eIF2 α phosphorylation, so the effect of CReP turnover was only subtle. This may reflect a greater need for this pathway in fast-growing cells, or the fact that these primary cells were under constant stress.

Upon proteostatic stress, eIF2 α phosphorylation promotes the translation of the transcription factor ATF4 [48]. ATF4 activates the expression of the transcription factor CHOP [48], which in turn promotes the transcription of GADD34 [49]. Like CReP, GADD34 is a PP1 targeting subunit that acts on Ser51 of eIF2 α [50,51]. These PP1 subunits appear to have a dedicated role in regulating eIF2 α , since the lethal phenotype of knockout mice lacking both GADD34 and CReP can be rescued by mutating eIF2 α Ser51 [50]. Previous reports suggested that GADD34 is induced at late time points after DNA damage in some cell types [52]. We were especially interested in whether DNA damage promoted the destruction of CReP only to replace it with GADD34. However, we found that UV treatment did not promote GADD34 protein expression, while ER stress induced by thapsigargin did (Fig 6A). This may reflect a cell-type difference between HEK293 cells and cells previously used to show GADD34 induction. Surprisingly, treating cells with UV and thapsigargin simultaneously blocked the thapsigargin-mediated increase in GADD34 protein levels, suggesting that DNA damage somehow dominantly prevents expression of this protein. Inhibition of GADD34 expression by UV treatment could be rescued by simultaneously treating cells with MLN4924, suggesting that a CRL is involved in blocking GADD34 accumulation.

Finally, we examined whether CReP turnover after DNA damage affected rates of translation. After treatment with DNA damage, translation rate was assayed via the SUnSET method [53], by adding puromycin to the cells for 10 minutes, then detecting the degree of puromycin incorporation into newly translating polypeptides via western blotting with an anti-puromycin antibody. We found that expression of CReP^{31A}, which led to high CReP levels even

after treatment with camptothecin and initial recovery from this damage, accelerated the recovery of translation after DNA damage, doubling the translation rate at 2 hours after CPT washout (Figs 6B and 6C). Notably, this effect was not seen with the unstable, ectopically expressed wildtype CReP, although it was expressed at the same level as CReP^{31A}. This effect reproduced several times, although the exact timing varies, likely due to subtle variations in CReP expression levels during transfection.

Discussion

We have identified and validated thirteen novel substrates of the well-studied ubiquitin ligase β TRCP via Ubiquitin Ligase Trapping. While we were unable to test two of the twenty-eight candidate substrates identified, 88% of the remaining twenty-six were either known or validated novel substrates. While affinity chromatography is often able to identify ligase substrates, these data suggest that Ligase Trapping provides an unprecedented hit rate, making it an especially efficient way to identify new ubiquitin ligase substrates. Moreover, this technology has allowed us to easily validate substrates even if their bulk stability is not affected by β TRCP ubiquitination.

Our results for FBW7 suggest another way in which Ligase Trapping can complement currently available techniques. In a previous study, the Clurman lab pulled out all 26 members of the Mediator complex with FBW7. They used degron prediction and follow-up experiments to identify MED13 and MED13L as the ubiquitylated Fbw7 substrates and carefully confirmed that they are direct substrates. Our mass spec of the Fbw7 ligase trap immunoprecipitation specifically purified MED13 (and MED13L) uniquely in the Fbw7 Ligase Trap, and not in any of the other purifications. Moreover, we pulled out none of the other 25 subunits. This underscores the usefulness of our technique, especially for the great majority of F box proteins for which no degron consensus is known. Thus, even in cases where Ligase Trapping identifies

similar numbers of substrates compared to other techniques, it allows one to quickly identify the directly ubiquitylated substrates.

In addition to the substrate CReP, which we followed up in detail, turnover of several of the other substrates is likely to be regulated in response to cell cycle position or stress. Sun2 is a transmembrane protein that spans the inner nuclear envelope and has been implicated in the maintenance of nuclear structure and the regulation of DNA damage. Its turnover by β TRCP may regulate these processes, and its removal from the membrane after ubiquitination may also be a regulated step. Strikingly, four of the eleven novel substrates we validated, ZNF395, HIVEP1/2, ZNF704, and AEBP2, are transcription factors, as are several known β TRCP substrates, such as Nrf2 and ATF4. We also identified two substrates that are themselves ubiquitin ligases, UBE4B and TRIM9, which opens up the possibility of complex mutual regulation. While UBE4B ubiquitination depends on the SCF (data not shown), it is not highly ubiquitinated (Figure 2), and it appears that the majority of the UBE4B population is stable (Figure 3B). RASSF3 is a candidate tumor suppressor protein that activates p53-dependent apoptosis under appropriate conditions, including DNA damage [54]. Its regulation by β TRCP is consistent with the known role of β TRCP in responding to DNA damage, and may help explain the oncogenic effect of β TRCP overexpression [18] (along with other known tumor suppressor substrates of β TRCP, such as REST[45]). RASSF3 appears to have both stable and unstable pools. This may reflect the relatively small pool of cells undergoing stress at any particular time in an untreated culture. Perturbations such as DNA damage might drive RASSF3 turnover.

Our previous studies in yeast [13] showed that 56% of newly-identified SCF substrates were strongly stabilized when the F box in question was mutated. 25% showed small or moderate stabilization, but were still unstable in the F box gene mutant. Finally, 19% appeared stable even in wildtype. We find here that 45% of confirmed novel substrates were stabilized by treatment with a pan-CRL inhibitor, 18% showed no stabilization, and 27% were stable in

wildtype. Thus, in both cases only half or fewer novel substrates were quantitatively turned over by the single ligase, although this is likely an underestimate overall, since previously characterized substrates may be biased for this category. While some of these effects could be due to the population assay employed, as noted above, substrates such as Cln3 and Gal4 in yeast, as well as PIP box-containing substrates in humans, are targeted in a way that is dependent upon the sub-cellular localization/context of the substrate [12,55]. Alternatively, some turnover events occur as part of quality control pathways that only target those proteins that are in some way defective.

We have implicated β TRCP in the regulation of translation initiation after DNA damage through its turnover of CReP, and shown that DNA damage-induced phosphorylation of eIF2 α , because it uniquely requires the depletion of CReP, occurs via a different mechanism from the other stresses known to promote eIF2 α phosphorylation, which all promote kinase activation. Previous work has shown that the phosphorylation of eIF2 α after UV treatment depends on the kinase Gcn2 [56,57]. We propose that this phosphorylation requires both Gcn2 activation and CReP turnover.

Why does phosphorylation of eIF2 α require CReP depletion after DNA damage, but not in response to proteostatic stress? One possibility is that eIF2 α kinases are less active after DNA damage than after proteostatic stress. We observed that, once CReP levels begin to drop, eIF2 α phosphorylation is much higher upon our UV treatment than after proteostatic stress (Fig 5A). This likely reflects both continued CReP activity and the induction of GADD34 upon proteostatic stress. We showed in Figs 6B and 6C that CReP turnover has a significant effect on translation rates after DNA damage, but substantial inhibition of translation happens even in the absence of CReP turnover. Translation rates are highly redundantly regulated, both via control of eIF2 α phosphorylation and via regulation of eIF4. Our results are consistent with a model in which CReP turnover is important to enforce continued low levels of translation at later

timepoints. Moreover, the high levels of eIF2 α phosphorylation enabled by CReP turnover in response to DNA damage may allow translational reprogramming that leads to induction of DNA damage repair proteins, even as global translation is downregulated. Indeed, translation of several DNA repair proteins has been shown to be resistant to inhibition of CAP-dependent translational inhibition by eIF2 α phosphorylation [57].

Finally, how do CRLs prevent the induction of GADD34 after UV treatment? One possibility is that CReP turnover upon DNA damage (which requires CRLs) drives such strong eIF2 α phosphorylation that translation of GADD34 or one of its upstream regulators ATF4 or CHOP is inhibited. Another possibility is that a CRL is turning over a specific protein to keep GADD34 levels low. β TRCP is known to target ATF4 [24] and the Cul3-associated ligase SPOP is reported to target CHOP [58]. GADD34 is also a known proteasome target, consistent with its being a substrate of β TRCP or another CRL [59]. Targeting of both CReP and Gadd34 for degradation upon DNA damage underscores the importance of limiting eIF2 α phosphatase activity during DNA damage.

Methods

Plasmids and tissue culture

All plasmids were transfected into the 293 FlpIn TRex cell line (Life Technologies, Grand Island, NY, USA), which contains both a site for FRT-mediated recombination (which we did not use in this work) and expresses the *tet* repressor, which allows doxycycline-inducible expression from promoters that include *tet* operators. Mouse embryonic fibroblasts (MEFs) were immortalized by transduction with the SV40 large T antigen (kind gift of Morgan Truitt and Davide Ruggero). All cells were grown in DMEM with 10% heat-inactivated fetal bovine serum. For large-scale purifications, medium was supplemented with 500 U/mL penicillin and 500 μ g/mL streptomycin.

6xHis-ubiquitin was expressed from pTB30, a modified pcDNA3.1 vector with a pCMV/TetO promoter expressing 6xHis-Uba52-IRES-6xHis-RPS27A. The parent of this construct was the kind gift of Zhijian Chen, UT Southwestern. The construct was linearized with *Pvu I* and transfected into 293 FlpIn TRex cells. Stable transfectants were selected with G418 and a clone was selected that expressed at a high level only upon treatment with doxycycline.

To make the ligase trap fusion proteins, F box proteins were fused on the C-terminus to 3xFlag followed by the C terminal half of human RAD23B (Accession #BC020973.2, amino acids 185-410), encoding two UBA domains. Ligase traps β TRCP2 (FBXW11; Accession #BC026213.1, pTB53), Fbxo24 (Accession #NM033506.2, pBEN20), and Fbxo6 (Accession #NM018438.5, pBEN5) were expressed as hygromycin resistance-T2A-ligase trap fusions driven by the mouse PGK1 promoter. Each of these constructs also expresses an shRNA against the relevant F box protein (to which the fusion protein is resistant), driven by the mouse U6 promoter. These cassettes were linearized by digestion with *Pac I*. Fbw7 (Accession# NM_033632.3, pTB59) Ligase Trap was expressed from a pcDNA3.1 vector, under the control of the CMV promoter. The vector was linearized with *BglIII*. All linearized plasmids were transfected into the HisUb cell line and stable transfectants were selected with hygromycin. We selected clonal cell lines that expressed moderate levels of the relevant ligase trap.

All substrate proteins were tagged on the N-terminus with the 5xHA epitope, and expressed from the CMV promoter in pcDNA3.1, except SUN2, AEBP2, ALDH2, and RASSF3, which were tagged on the C-terminus. They were transiently transfected into the relevant cell line using Fugene HD at 3 μ L/ μ g DNA (Promega Corporation, Madison, WI, USA) or polyethyleneimine (at 18 μ g/ μ g DNA) 24-48 hours before the experiment. β TRCP was knocked down with an shRNA targeting both BTRC and FBXW11, expressed from the pSUPER-puro-retro vector (under the H1 promoter)[60].

Drugs

MG132 is used at 5 μ M. MLN4924 is used at 1 μ M. Camptothecin is used at 3 μ g/mL, unless otherwise specified.

UV treatment

Medium was removed from adherent cells and set aside. Cells were covered in 37°C 1X PBS with 0.9 mM CaCl₂ and 0.5 mM MgCl₂, then exposed to 300 J/m² UV-C, PBS was aspirated, and medium was replaced.

Antibodies and western blotting

For western blotting, cells were lysed in 1X RIPA buffer with protease and phosphatase inhibitors for 30 minutes on ice, insoluble material was spun out, then protein concentrations were measured with BCA Reagent (Pierce, Thermo Scientific, Rockford, IL, USA) and normalized before addition of SDS sample buffer with DTT. For Figures S7 (except for RASSF3) and 5C, cells were lysed directly in SDS sample buffer with DTT or β Me.

All gels were Criterion Tris-HCl 4-20% gradients (cat. #345-0034, BioRad, Hercules, CA, USA), except for the gel for the α -HA blot in Figure 2C, which was a 7.5% gel (BioRad cat. #345-0007).

Antibodies used were α -HA 16B12 at 1:1,000-1:2,000 (cat. #MMS-101R, Covance, Emeryville, CA, USA), α -6xHis at 1:1,000-1:2,000, α -ubiquitin P4D1 at 1:100, α -Flag M2 at 1:2,000 (cat. #F3165, Sigma, St. Louis, MO, USA), α -Cul1 at 1:1,000, α -vinculin at 1:1,000-1:5,000, α - β actin at 1:1,000-1:10,000 (Sigma cat. #A5441 for Figure 4A, Abcam, Cambridge, UK, cat.#ab8226 for all others), α -PPP1R15B (CReP) at 1:1,000-1:5,000 (cat. #14634-1-AP, Proteintech, Chicago, IL, USA), and α -GADD34 (cat. # 10449-1-AP, Proteintech, Chicago, IL, USA). α -phosphoS51-eIF2 α (cat. #9721), α -eIF2 α (cat. #9722), α -phosphoS317Chk1 (cat. #2344), and α -Chk1 (cat. #2360) antibodies were all from Cell Signaling Technologies, Danvers, MA, USA. The α -puromycin antibody 12D10 was from EMD Millipore (cat. #MABE343).

Western blots in Figures 1, 2A-B, and 3A were incubated with secondary antibodies fused to horseradish peroxidase and visualized by treatment with Western Lightning ECL (Perkin Elmer, Waltham, MA, USA). Western blots in Figures 2C, 3B, and Figure 4 were incubated with fluorescent secondary antibodies and visualized with an Odyssey scanner (Licor, Lincoln, NE, USA).

Immunoprecipitations of Ligase Traps

Unless otherwise noted, stable cell lines expressing Ligase Traps were treated with 5 μ M MG132 for 4 hours before collection. We grew 100-200 barely sub-confluent 15 cm dishes for each purification, representing approximately $1-3 \times 10^9$ cells. Pellets were lysed in 25 mM Hepes-KOH, pH8, 150 mM K Oac, 10 mM MgCl₂, 5 mM CaCl₂, 20 mM iodoacetamide, 30 μ M MG132, protease inhibitors, and phosphatase inhibitors by sonication, then treated with DNase (660 U/mL) at 4°C for 30 minutes before addition of Nonidet P-40 to 0.1%. Samples were spun to remove insoluble material, then incubated with α -Flag M2 magnetic beads (Sigma, St. Louis, MO, USA) at 4°C overnight. Beads were washed 5 times in 1X PBS+0.1% Nonidet P-40, then eluted in this wash buffer+0.5 mg/mL 3xFlag peptide. The eluate was denatured by addition of 2X volume Buffer B (216 mM NaH₂PO₄, 16 mM Tris, 9.37 M urea, pHed to 8). The sample was then incubated with NiNTA agarose for 3 hours at room temperature. The beads were washed 3X in Buffer B diluted to 8M urea+10 mM imidazole, then 2X in Buffer B diluted to 1 M urea+10mM imidazole. Samples were eluted in 0.5 M urea, 300 mM imidazole, 0.1% rapigest (or Nonidet P-40 if not to be used for mass spectrometry), 108 mM NaH₂PO₄, 8 mM Tris (pHed to 8 before adding imidazole).

Mass Spectrometry analysis

The immunopurified protein complexes were mixed in a ratio of 1:1 with digestion buffer (100 mM Tris-HCl, pH 8.5, 8M urea), reduced, alkylated and digested by sequential addition of

lys-C and trypsin proteases as previously described[61,62]. For identification of phosphorylation site, proteins were digested directly in the excised gel slice using trypsin[61]. Peptide digests desalted and fractionated online using a 50 μ M inner diameter fritted fused silica capillary column with a 5 μ M pulled electrospray tip and packed in-house with 15 cm of Luna C18(2) 3 μ M reversed phase particles. The gradient was delivered by an easy-nLC 1000 ultra high pressure chromatography system (Thermo Scientific). MS/MS spectra were collected on a Q-Exactive mass spectrometer (Thermo Scientific) [63,64]. Data analysis was performed using the ProLuCID, DTASelect2, and Ascore algorithms as implemented in the Integrated Proteomics Pipeline - IP2 (Integrated Proteomics Applications, Inc., San Diego, CA) [65-68].

Phosphopeptides were identified using a differential modification search that considered a mass shift of +79.9663 on serines, threonines and tyrosines. Protein and peptide identifications were filtered using DTASelect and required at least two unique peptides per protein and a peptide-level false positive rate of less than 5% as estimated by a decoy database strategy[69].

Normalized spectral abundance factor (NSAF) values were calculated as described and multiplied by 10^5 to improve readability [70].

Puromycin incorporation assay

We followed the SUnSET protocol [53]. Puromycin was added to culture medium at a final concentration of 10 μ g/mL, incubated for 10 minutes at 37°C and 8% CO₂, then medium was replaced with ice-cold PBS with 5 mM EDTA, and cells were sprayed from the dish on ice, spun down at 4°C and flash-frozen. Samples were normalized by protein concentration, and puromycin incorporation was detected by western blotting with a monoclonal anti-puromycin antibody (12D10) and quantified by densitometry.

Acknowledgements

We thank Zhijian J. Chen, Nikita Popov, Martin Eilers, Randal Kaufman, Morgan Truitt, and Davide Ruggero for gifts of reagents; members of T.B.L.'s thesis committee and of the Toczyski and Ruggero labs for helpful discussions; and Jessica Lao for critical reading of the manuscript.

References

1. Benanti JA, Cheung SK, Brady MC, Toczyski DP (2007) A proteomic screen reveals SCFGrr1 targets that regulate the glycolytic-gluconeogenic switch. *Nat Cell Biol* 9: 1184-1191.
2. Yen HC, Elledge SJ (2008) Identification of SCF ubiquitin ligase substrates by global protein stability profiling. *Science* 322: 923-929.
3. Yen HC, Xu Q, Chou DM, Zhao Z, Elledge SJ (2008) Global protein stability profiling in mammalian cells. *Science* 322: 918-923.
4. Emanuele MJ, Elia AE, Xu Q, Thoma CR, Izhar L, et al. (2011) Global identification of modular cullin-RING ligase substrates. *Cell* 147: 459-474.
5. Kim W, Bennett EJ, Huttlin EL, Guo A, Li J, et al. (2011) Systematic and quantitative assessment of the ubiquitin-modified proteome. *Mol Cell* 44: 325-340.
6. Dorrello NV, Peschiaroli A, Guardavaccaro D, Colburn NH, Sherman NE, et al. (2006) S6K1- and betaTRCP-mediated degradation of PDCD4 promotes protein translation and cell growth. *Science* 314: 467-471.
7. Peschiaroli A, Dorrello NV, Guardavaccaro D, Venere M, Halazonetis T, et al. (2006) SCFbetaTrCP-mediated degradation of Claspin regulates recovery from the DNA replication checkpoint response. *Mol Cell* 23: 319-329.
8. Sowa ME, Bennett EJ, Gygi SP, Harper JW (2009) Defining the human deubiquitinating enzyme interaction landscape. *Cell* 138: 389-403.
9. Vashisht AA, Zumbrennen KB, Huang X, Powers DN, Durazo A, et al. (2009) Control of iron homeostasis by an iron-regulated ubiquitin ligase. *Science* 326: 718-721.

10. Davis MA, Larimore EA, Fissel BM, Swanger J, Taatjes DJ, et al. (2013) The SCF-Fbw7 ubiquitin ligase degrades MED13 and MED13L and regulates CDK8 module association with Mediator. *Genes Dev* 27: 151-156.
11. Tan MK, Lim HJ, Bennett EJ, Shi Y, Harper JW (2013) Parallel SCF adaptor capture proteomics reveals a role for SCFFBXL17 in NRF2 activation via BACH1 repressor turnover. *Mol Cell* 52: 9-24.
12. Landry BD, Doyle JP, Toczyski DP, Benanti JA (2012) F-box protein specificity for G1 cyclins is dictated by subcellular localization. *PLoS Genet* 8: e1002851.
13. Mark KG, Simonetta M, Maiolica A, Seller CA, Toczyski DP (2014) Ubiquitin ligase trapping identifies an SCF(Saf1) pathway targeting unprocessed vacuolar/lysosomal proteins. *Mol Cell* 53: 148-161.
14. Skaar JR, Pagan JK, Pagano M (2013) Mechanisms and function of substrate recruitment by F-box proteins. *Nat Rev Mol Cell Biol* 14: 369-381.
15. Willems AR, Schwab M, Tyers M (2004) A hitchhiker's guide to the cullin ubiquitin ligases: SCF and its kin. *Biochim Biophys Acta* 1695: 133-170.
16. Deshaies RJ (1999) SCF and Cullin/Ring H2-based ubiquitin ligases. *Annu Rev Cell Dev Biol* 15: 435-467.
17. Reed SI (2006) The ubiquitin-proteasome pathway in cell cycle control. *Results Probl Cell Differ* 42: 147-181.
18. Frescas D, Pagano M (2008) Deregulated proteolysis by the F-box proteins SKP2 and beta-TrCP: tipping the scales of cancer. *Nat Rev Cancer* 8: 438-449.
19. Watanabe N, Arai H, Nishihara Y, Taniguchi M, Watanabe N, et al. (2004) M-phase kinases induce phospho-dependent ubiquitination of somatic Wee1 by SCFbeta-TrCP. *Proc Natl Acad Sci U S A* 101: 4419-4424.

20. Busino L, Donzelli M, Chiesa M, Guardavaccaro D, Ganoth D, et al. (2003) Degradation of Cdc25A by beta-TrCP during S phase and in response to DNA damage. *Nature* 426: 87-91.
21. Jin J, Shirogane T, Xu L, Nalepa G, Qin J, et al. (2003) SCFbeta-TRCP links Chk1 signaling to degradation of the Cdc25A protein phosphatase. *Genes Dev* 17: 3062-3074.
22. Mamely I, van Vugt MA, Smits VA, Semple JI, Lemmens B, et al. (2006) Polo-like kinase-1 controls proteasome-dependent degradation of Claspin during checkpoint recovery. *Curr Biol* 16: 1950-1955.
23. Rada P, Rojo AI, Chowdhry S, McMahon M, Hayes JD, et al. (2011) SCF/{beta}-TrCP promotes glycogen synthase kinase 3-dependent degradation of the Nrf2 transcription factor in a Keap1-independent manner. *Mol Cell Biol* 31: 1121-1133.
24. Lassot I, Segeral E, Berlioz-Torrent C, Durand H, Groussin L, et al. (2001) ATF4 degradation relies on a phosphorylation-dependent interaction with the SCF(betaTrCP) ubiquitin ligase. *Mol Cell Biol* 21: 2192-2202.
25. Kanemori Y, Uto K, Sagata N (2005) Beta-TrCP recognizes a previously undescribed nonphosphorylated destruction motif in Cdc25A and Cdc25B phosphatases. *Proc Natl Acad Sci U S A* 102: 6279-6284.
26. Uchida S, Watanabe N, Kudo Y, Yoshioka K, Matsunaga T, et al. (2011) SCFbeta(TrCP) mediates stress-activated MAPK-induced Cdc25B degradation. *J Cell Sci* 124: 2816-2825.
27. Wang Z, Zhong J, Gao D, Inuzuka H, Liu P, et al. (2012) DEPTOR ubiquitination and destruction by SCF(beta-TrCP). *Am J Physiol Endocrinol Metab* 303: E163-169.
28. Magliozzi R, Low TY, Weijts BG, Cheng T, Spanjaard E, et al. (2013) Control of epithelial cell migration and invasion by the IKKbeta- and CK1alpha-mediated degradation of RAPGEF2. *Dev Cell* 27: 574-585.

29. Margottin-Goguet F, Hsu JY, Loktev A, Hsieh HM, Reimann JD, et al. (2003) Prophase destruction of Emi1 by the SCF(betaTrCP/Slimb) ubiquitin ligase activates the anaphase promoting complex to allow progression beyond prometaphase. *Dev Cell* 4: 813-826.
30. Yang X, Wood PA, Ansell CM, Ohmori M, Oh EY, et al. (2009) Beta-catenin induces beta-TrCP-mediated PER2 degradation altering circadian clock gene expression in intestinal mucosa of ApcMin/+ mice. *J Biochem* 145: 289-297.
31. Huang W, Lv X, Liu C, Zha Z, Zhang H, et al. (2012) The N-terminal phosphodegron targets TAZ/WWTR1 protein for SCFbeta-TrCP-dependent degradation in response to phosphatidylinositol 3-kinase inhibition. *J Biol Chem* 287: 26245-26253.
32. D'Annibale S, Kim J, Magliozzi R, Low TY, Mohammed S, et al. (2014) Proteasome-dependent degradation of transcription factor activating enhancer-binding protein 4 (TFAP4) controls mitotic division. *J Biol Chem* 289: 7730-7737.
33. Kim J, D'Annibale S, Magliozzi R, Low TY, Jansen P, et al. (2014) USP17- and SCFbetaTrCP--regulated degradation of DEC1 controls the DNA damage response. *Mol Cell Biol* 34: 4177-4185.
34. Jousse C, Oyadomari S, Novoa I, Lu P, Zhang Y, et al. (2003) Inhibition of a constitutive translation initiation factor 2alpha phosphatase, CReP, promotes survival of stressed cells. *J Cell Biol* 163: 767-775.
35. Pavitt GD, Ron D (2012) New insights into translational regulation in the endoplasmic reticulum unfolded protein response. *Cold Spring Harb Perspect Biol* 4.
36. Holcik M, Sonenberg N (2005) Translational control in stress and apoptosis. *Nat Rev Mol Cell Biol* 6: 318-327.
37. Wu G, Xu G, Schulman BA, Jeffrey PD, Harper JW, et al. (2003) Structure of a beta-TrCP1-Skp1-beta-catenin complex: destruction motif binding and lysine specificity of the SCF(beta-TrCP1) ubiquitin ligase. *Mol Cell* 11: 1445-1456.

38. Rual JF, Venkatesan K, Hao T, Hirozane-Kishikawa T, Dricot A, et al. (2005) Towards a proteome-scale map of the human protein-protein interaction network. *Nature* 437: 1173-1178.
39. Kim TY, Siesser PF, Rossman KL, Goldfarb D, Mackinnon K, et al. (2015) Substrate Trapping Proteomics Reveals Targets of the betaTrCP2/FBXW11 Ubiquitin Ligase. *Mol Cell Biol* 35: 167-181.
40. Low TY, Peng M, Magliozzi R, Mohammed S, Guardavaccaro D, et al. (2014) A systems-wide screen identifies substrates of the SCFbetaTrCP ubiquitin ligase. *Sci Signal* 7: rs8.
41. Latres E, Chiaur DS, Pagano M (1999) The human F box protein beta-Trcp associates with the Cul1/Skp1 complex and regulates the stability of beta-catenin. *Oncogene* 18: 849-854.
42. Qu Z, Qing G, Rabson A, Xiao G (2004) Tax deregulation of NF-kappaB2 p100 processing involves both beta-TrCP-dependent and -independent mechanisms. *J Biol Chem* 279: 44563-44572.
43. Kruiswijk F, Yuniati L, Magliozzi R, Low TY, Lim R, et al. (2012) Coupled activation and degradation of eEF2K regulates protein synthesis in response to genotoxic stress. *Sci Signal* 5: ra40.
44. Guardavaccaro D, Frescas D, Dorrello NV, Peschiaroli A, Multani AS, et al. (2008) Control of chromosome stability by the beta-TrCP-REST-Mad2 axis. *Nature* 452: 365-369.
45. Westbrook TF, Hu G, Ang XL, Mulligan P, Pavlova NN, et al. (2008) SCFbeta-TRCP controls oncogenic transformation and neural differentiation through REST degradation. *Nature* 452: 370-374.
46. Paul M, Jabbar MA (1997) Phosphorylation of both phosphoacceptor sites in the HIV-1 Vpu cytoplasmic domain is essential for Vpu-mediated ER degradation of CD4. *Virology* 232: 207-216.

47. Coyaud E, Mis M, Laurent EM, Dunham WH, Couzens AL, et al. (2015) BioID-based identification of SCF beta-TrCP1/2 E3 ligase substrates. *Mol Cell Proteomics*.
48. Harding HP, Novoa I, Zhang Y, Zeng H, Wek R, et al. (2000) Regulated translation initiation controls stress-induced gene expression in mammalian cells. *Mol Cell* 6: 1099-1108.
49. Marciniak SJ, Yun CY, Oyadomari S, Novoa I, Zhang Y, et al. (2004) CHOP induces death by promoting protein synthesis and oxidation in the stressed endoplasmic reticulum. *Genes Dev* 18: 3066-3077.
50. Harding HP, Zhang Y, Scheuner D, Chen JJ, Kaufman RJ, et al. (2009) Ppp1r15 gene knockout reveals an essential role for translation initiation factor 2 alpha (eIF2alpha) dephosphorylation in mammalian development. *Proc Natl Acad Sci U S A* 106: 1832-1837.
51. Novoa I, Zeng H, Harding HP, Ron D (2001) Feedback inhibition of the unfolded protein response by GADD34-mediated dephosphorylation of eIF2alpha. *J Cell Biol* 153: 1011-1022.
52. Fornace AJ, Jr., Jackman J, Hollander MC, Hoffman-Liebermann B, Liebermann DA (1992) Genotoxic-stress-response genes and growth-arrest genes. gadd, MyD, and other genes induced by treatments eliciting growth arrest. *Ann N Y Acad Sci* 663: 139-153.
53. Schmidt EK, Clavarino G, Ceppi M, Pierre P (2009) SUnSET, a nonradioactive method to monitor protein synthesis. *Nat Methods* 6: 275-277.
54. Kudo T, Ikeda M, Nishikawa M, Yang Z, Ohno K, et al. (2012) The RASSF3 candidate tumor suppressor induces apoptosis and G1-S cell-cycle arrest via p53. *Cancer Res* 72: 2901-2911.
55. Muratani M, Kung C, Shokat KM, Tansey WP (2005) The F box protein Dsg1/Mdm30 is a transcriptional coactivator that stimulates Gal4 turnover and cotranscriptional mRNA processing. *Cell* 120: 887-899.

56. Deng J, Harding HP, Raught B, Gingras AC, Berlanga JJ, et al. (2002) Activation of GCN2 in UV-irradiated cells inhibits translation. *Curr Biol* 12: 1279-1286.
57. Powley IR, Kondrashov A, Young LA, Dobbyn HC, Hill K, et al. (2009) Translational reprogramming following UVB irradiation is mediated by DNA-PKcs and allows selective recruitment to the polysomes of mRNAs encoding DNA repair enzymes. *Genes Dev* 23: 1207-1220.
58. Zhang P, Gao K, Tang Y, Jin X, An J, et al. (2014) Destruction of DDIT3/CHOP Protein by Wild-Type SPOP but Not Prostate Cancer-Associated Mutants. *Hum Mutat* 35: 1142-1151.
59. Brush MH, Shenolikar S (2008) Control of cellular GADD34 levels by the 26S proteasome. *Mol Cell Biol* 28: 6989-7000.
60. Popov N, Schulein C, Jaenicke LA, Eilers M (2010) Ubiquitylation of the amino terminus of Myc by SCF(beta-TrCP) antagonizes SCF(Fbw7)-mediated turnover. *Nat Cell Biol* 12: 973-981.
61. Kaiser P, Wohlschlegel J (2005) Identification of ubiquitination sites and determination of ubiquitin-chain architectures by mass spectrometry. *Methods in Enzymology* 399: 266-277.
62. Wohlschlegel JA (2009) Identification of SUMO-conjugated proteins and their SUMO attachment sites using proteomic mass spectrometry. *Methods in molecular biology* 497: 33-49.
63. Kelstrup CD, Young C, Lavalley R, Nielsen ML, Olsen JV (2012) Optimized fast and sensitive acquisition methods for shotgun proteomics on a quadrupole orbitrap mass spectrometer. *Journal of proteome research* 11: 3487-3497.
64. Michalski A, Damoc E, Hauschild JP, Lange O, Wiegand A, et al. (2011) Mass spectrometry-based proteomics using Q Exactive, a high-performance benchtop

- quadrupole Orbitrap mass spectrometer. *Molecular & cellular proteomics* : MCP 10: M111 011015.
65. Beausoleil SA, Villen J, Gerber SA, Rush J, Gygi SP (2006) A probability-based approach for high-throughput protein phosphorylation analysis and site localization. *Nature biotechnology* 24: 1285-1292.
 66. Cociorva D, D LT, Yates JR (2007) Validation of tandem mass spectrometry database search results using DTASelect. *Curr Protoc Bioinformatics* Chapter 13: Unit 13 14.
 67. Tabb DL, McDonald WH, Yates JR, 3rd (2002) DTASelect and Contrast: tools for assembling and comparing protein identifications from shotgun proteomics. *J Proteome Res* 1: 21-26.
 68. Xu T, Venable JD, Park SK, Cociorva D, Lu B, et al. (2006) ProLuCID, A Fast and Sensitive Tandem Mass Spectra-based Protein Identification Programs. *Molecular & Cellular Proteomics* 5: S174.
 69. Elias JE, Gygi SP (2007) Target-decoy search strategy for increased confidence in large-scale protein identifications by mass spectrometry. *Nat Methods* 4: 207-214.
 70. Florens L, Carozza MJ, Swanson SK, Fournier M, Coleman MK, et al. (2006) Analyzing chromatin remodeling complexes using shotgun proteomics and normalized spectral abundance factors. *Methods* 40: 303-311.

Figure Legends

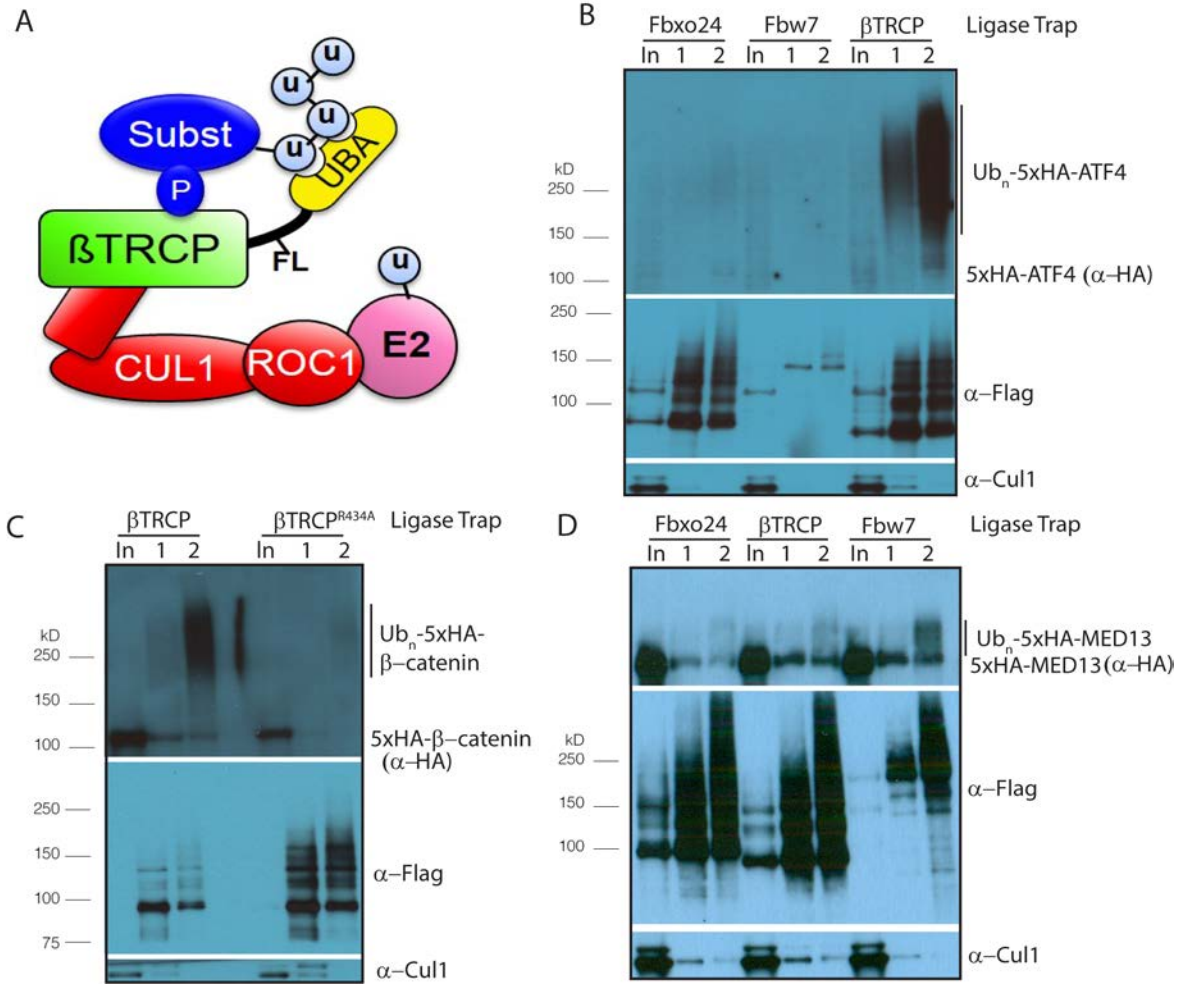


Fig 1. Establishing Ligase Trapping in human cells. (A) The SCF includes the scaffolds Skp1 (unlabeled, in red) and Cul1, which connect the E2-binding protein Roc1 to an F box protein such as βTRCP, which recruits substrates. Ligase Trapping is a two-step process in which ubiquitinated substrates are first precipitated under native conditions by a ubiquitin ligase fused to a UBA domain and then purified further under denaturing conditions via a 6xHis tag on ubiquitin. (B) βTRCP Ligase Trap purifies ubiquitinated species of the known substrate ATF4. Stable cell lines expressing the βTRCP Ligase Trap or a negative control (FBXO24 or Fbw7) were induced to express 6xHisUb for 3 days, transfected with 5xHA-tagged ATF4 for 24 hours, treated with 5 μM MG132 for 4 hours, lysed and subjected to a two-step precipitation. First, the Ligase Traps were purified under native conditions with anti-Flag antibody and eluted with Flag

peptide. Then, the eluate was denatured in 6M urea and ubiquitinated proteins purified with NiNTA beads and eluted with imidazole. Loading was 1X input (In), 250X 1st step (1), and 5,000X 2nd step (2). (C) The interaction between the β TRCP Ligase Trap and the known substrate β -catenin depends on conserved substrate-binding regions in β TRCP. The pull-down in B was repeated, but without MG132 and with the substrate β -catenin as prey and both wt and mutant β TRCP as bait. (D) Fbw7 Ligase Trap specifically purifies ubiquitinated species of the known Fbw7 substrate MED13. Performed as in Figure 1B.

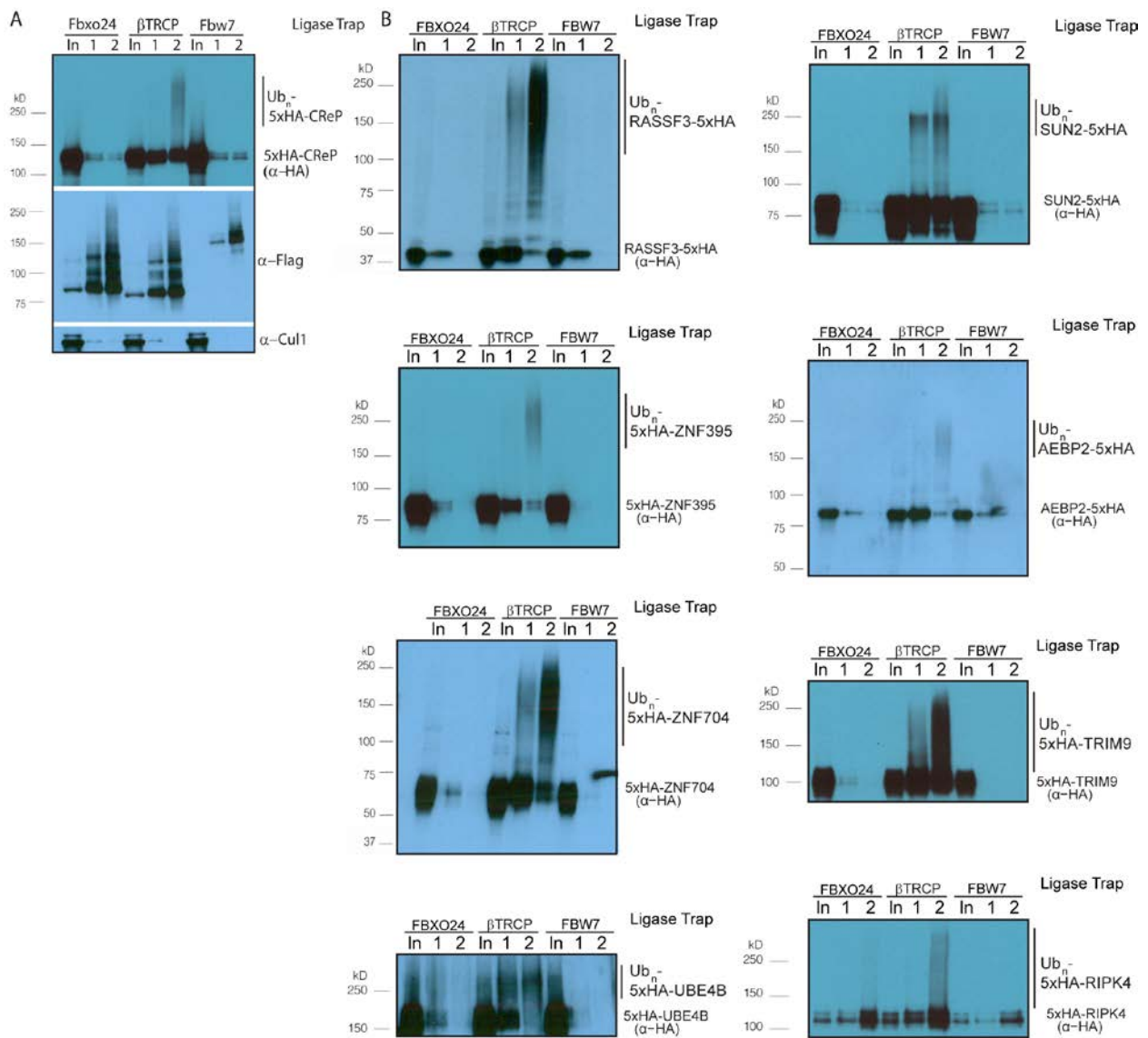


Fig 2. Validation of novel β TRCP substrates. (A) β TRCP Ligase Trap specifically purifies ubiquitinated species of the novel β TRCP substrate CReP. Performed as in Figure 1, without MG132 treatment. Loading was 1X for input, 250X for the 1st step, and 5,000X for the 2nd step. (B) Validation of additional candidate substrates. Loading controls and the rest of the substrates are in Figures S3 and S4.

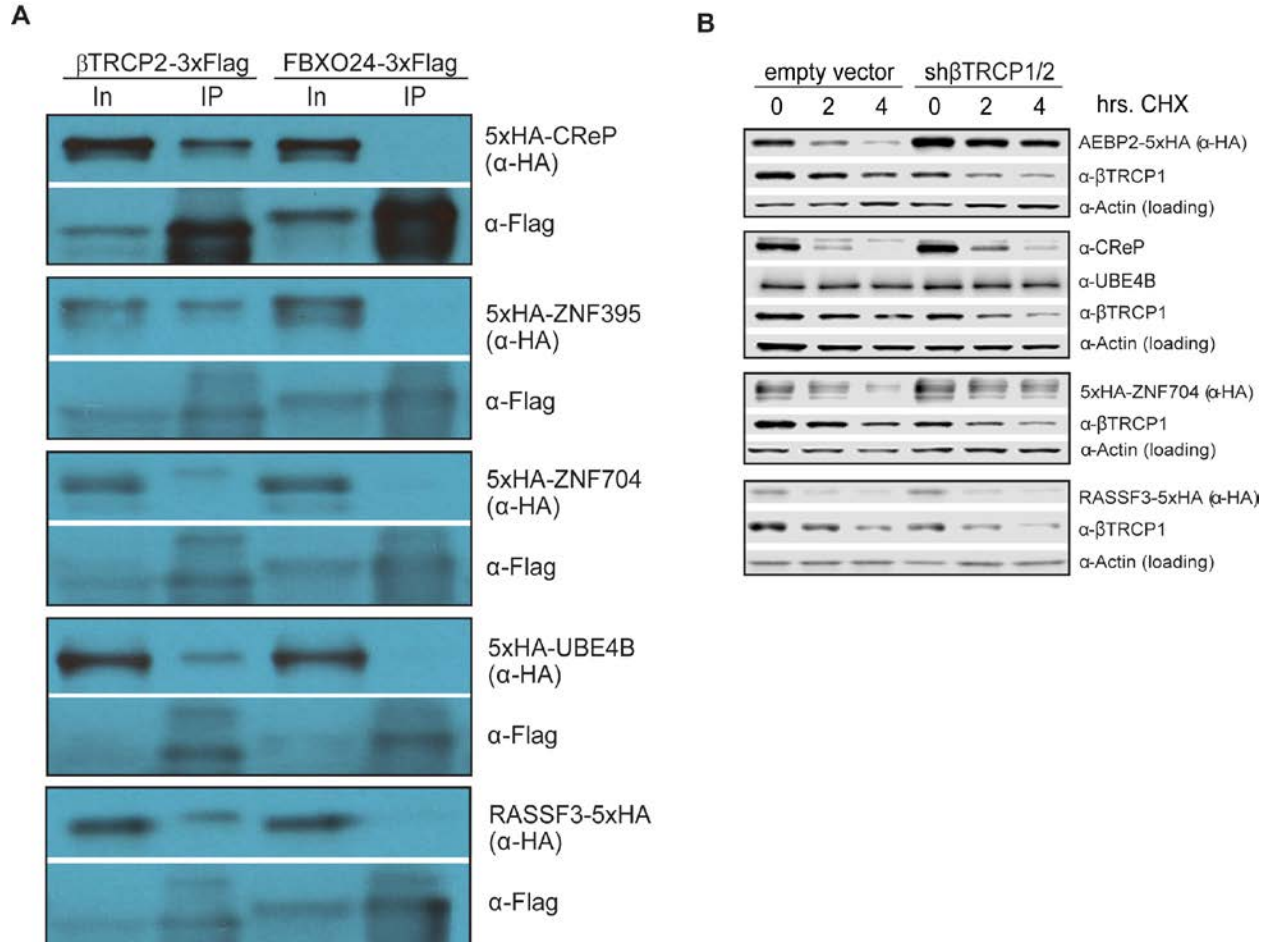


Fig 3. Ubiquitin ligase binding and turnover of a subset of novel β TRCP substrates. (A) β TRCP binds to its candidate substrates *in vivo*. HEK293 cells were transfected with 3xFlag-tagged F box proteins and 5xHA-tagged substrates for 1 day, lysed and subjected to a one-step precipitation. The F box proteins were purified under native conditions with anti-Flag antibody and eluted with Flag peptide. Loading was 1X input (In) and 75.3X IP for CReP, and 1X input (In) and 83.7X IP for other substrates. (B) Effect of β TRCP knockdown on candidate substrate

half-life. HEK293 cells were co-transfected with a negative control plasmid, or a plasmid encoding an shRNA targeting β TRCP1 and 2, and a plasmid encoding a tagged β TRCP candidate substrate. Cells were treated with 100 μ g/mL cycloheximide for the indicated time before collection.

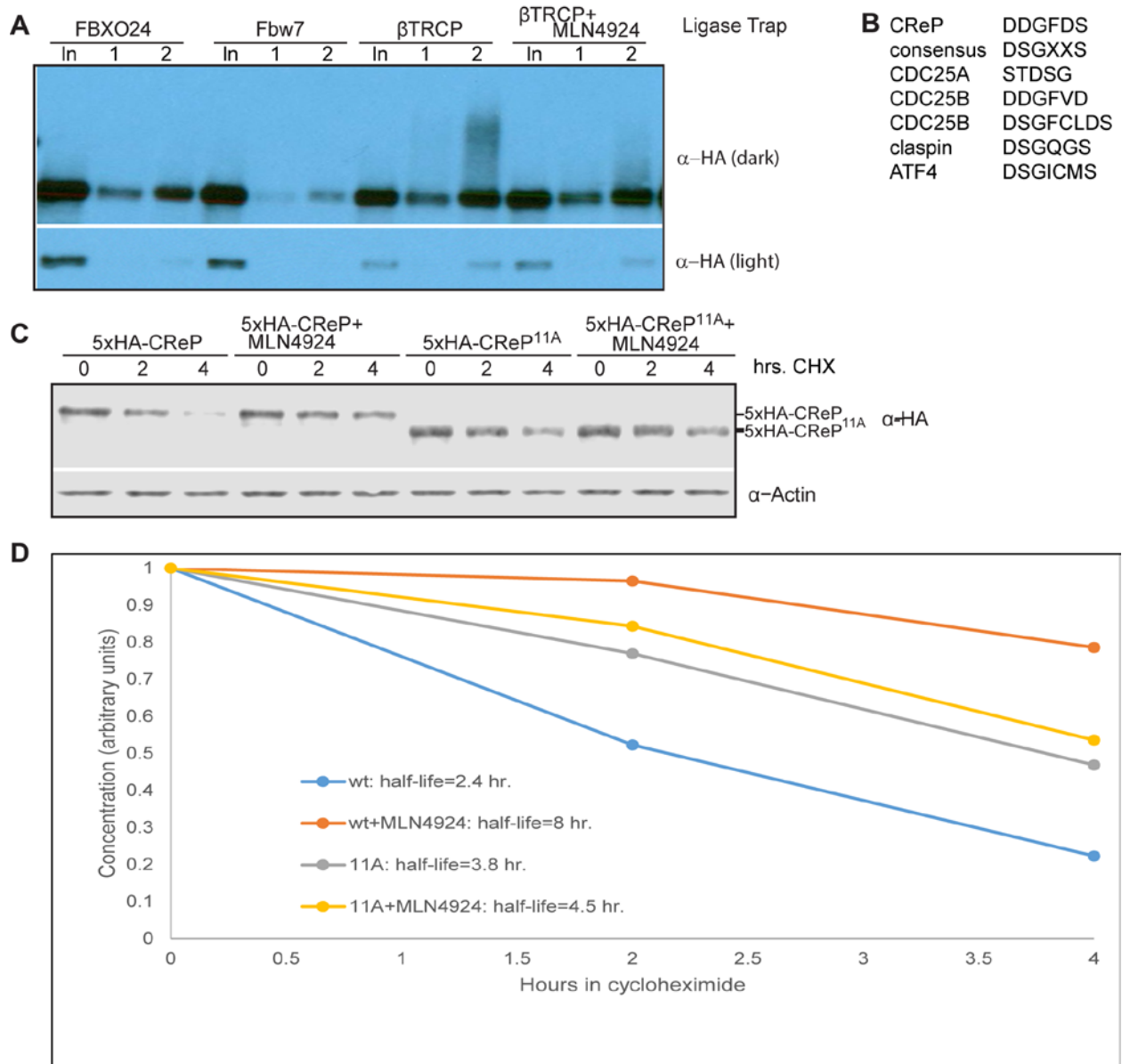


Fig 4. CReP ubiquitination is dependent on CRLs and turnover is regulated by a β TRCP consensus degron. (A) Ubiquitinated CReP precipitated by the β TRCP ligase trap depends on cullin activity. Tagged CReP was transiently expressed in the β TRCP or negative control ligase

trap cell lines, as in Figure 2B. Where indicated, 1 μ M MLN4924 was added 4 hours before cell collection to inhibit cullin activity. (B) A near-consensus β TRCP degron in CReP, compared to well-validated degrons. (C) CReP turnover depends on β TRCP consensus sites. Two consensus sites in CReP were mutated to generate the 11A mutant. Wildtype or mutant CReP was expressed transiently in 293 cells, which were then treated with 100 μ g/mL cycloheximide for the time indicated to monitor degradation in the absence of new protein synthesis. Where indicated, cells were treated with 1 μ M MLN4924 coincident with cycloheximide addition. (D) Quantitation of the average of two independent replicates of (B).

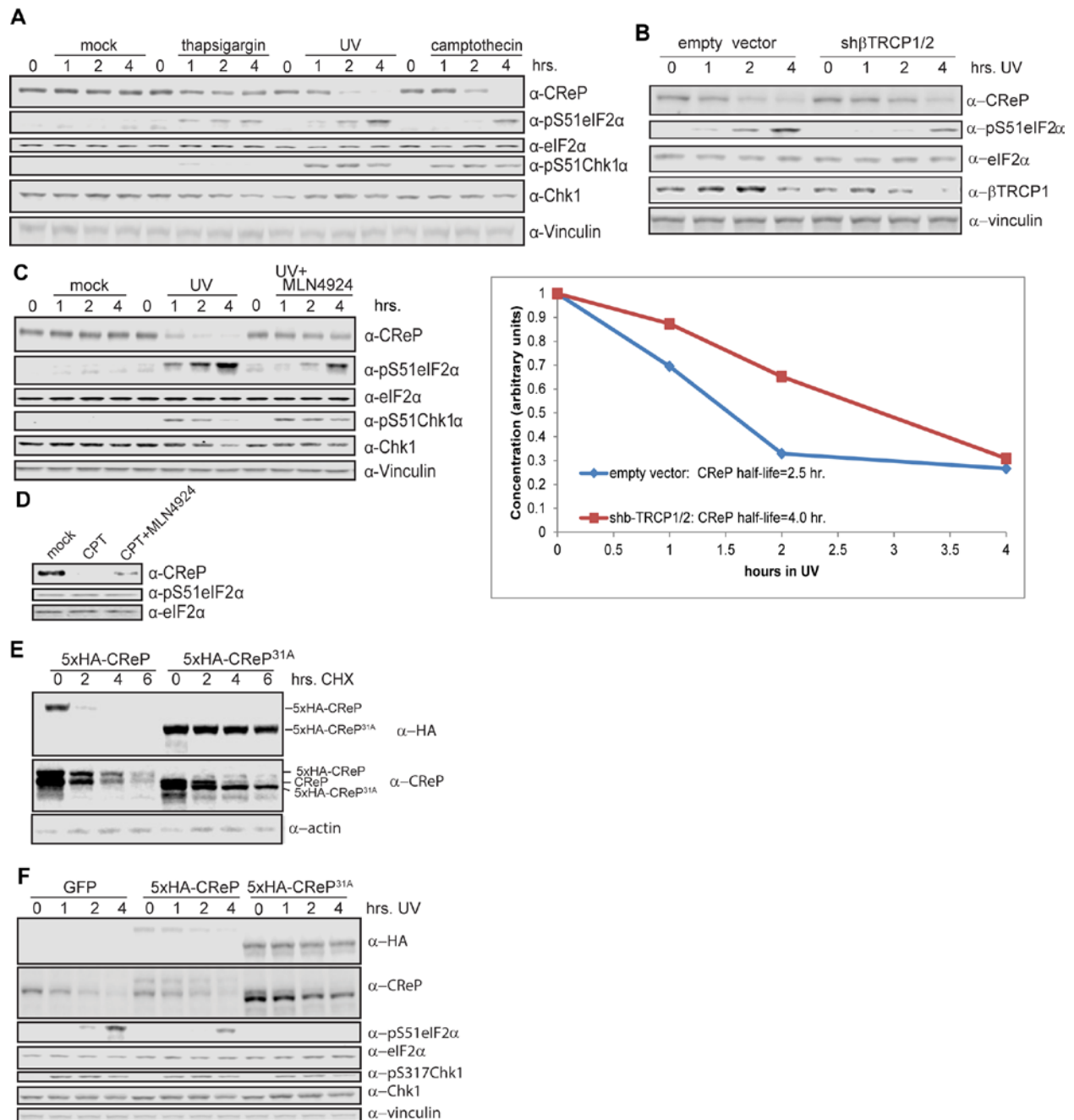


Fig 5. Regulation of CReP turnover and impact on eIF2α phosphorylation. (A) CReP is depleted upon DNA damage but not proteostatic stress. Cells were treated with 1 μM thapsigargin, 3 μg/mL camptothecin, or 300 J/m² UV for the indicated time; all samples not treated with UV were mock-treated and all samples were given the same total volume of the solvent DMSO. (B) CReP turnover upon DNA damage depends at least in part on βTRCP. Cells were transfected for 48 hours with an empty vector or shRNA targeting βTRCP1 and 2, then

irradiated with 300 J/m² UV-C. CReP levels are quantitated below, and the half-life calculated from the linear (0-2 hr.) part of the timecourse. (C) CReP depletion and full eIF2 α phosphorylation in UV depends on CRLs. Cells were treated with UV with or without MLN4924 for the times indicated. (D) CReP depletion in primary human fibroblasts depends on CRLs. Primary human fibroblasts were treated with 1 μ g/mL camptothecin for 6 hours, with 1 μ M MLN4924 where indicated. (E) The 31A allele of CReP is stable even upon treatment with DNA damage and cycloheximide. Cells were transfected with wildtype or mutant CReP, then pre-treated for 2 hours with 3 μ g/mL camptothecin before addition of cycloheximide. (F) Expression of a stable allele of CReP prevents phosphorylation of eIF2 α in response to UV treatment. Cells were transfected with tagged wild type or mutant CReP, then treated with UV for the indicated times.

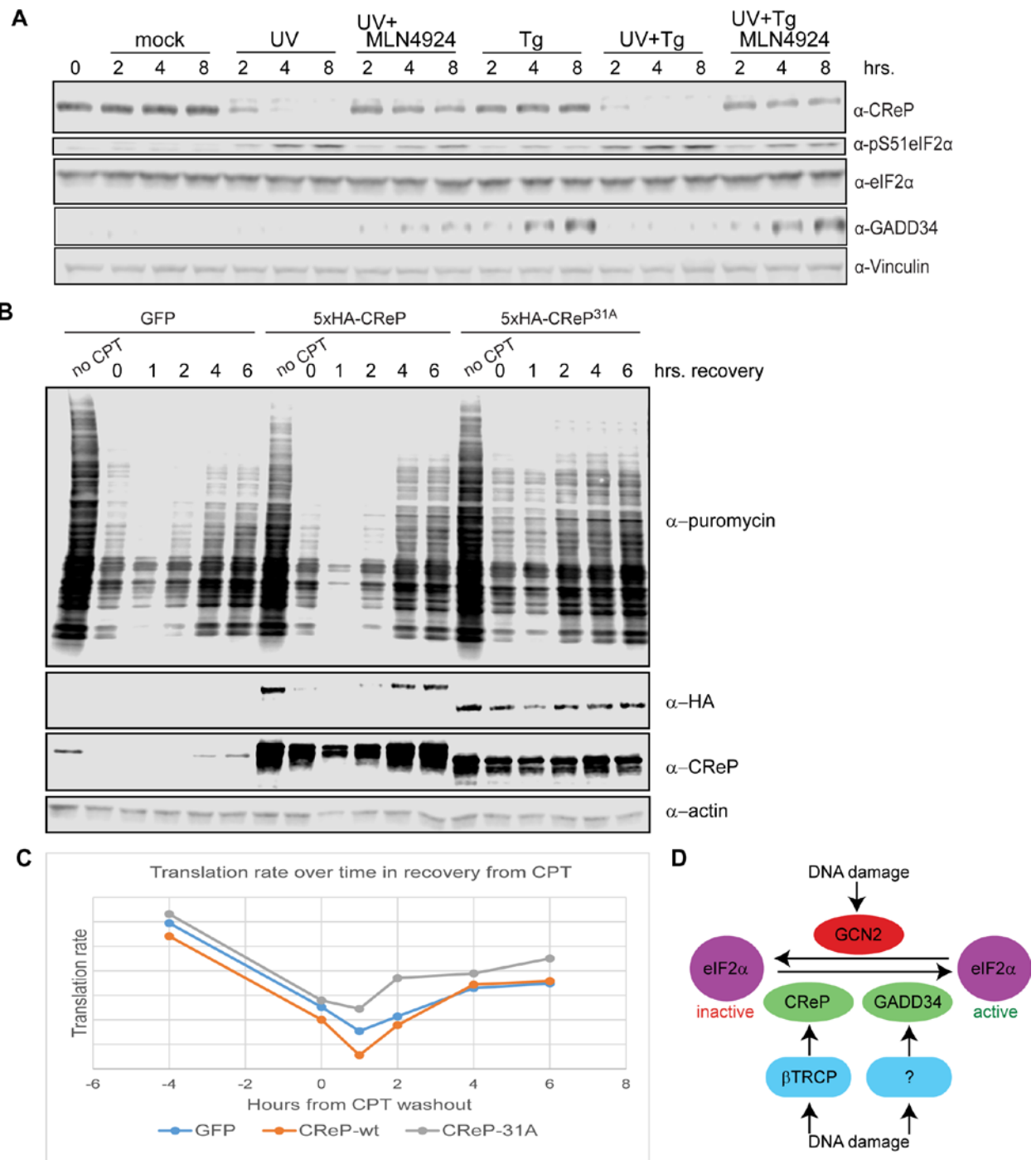
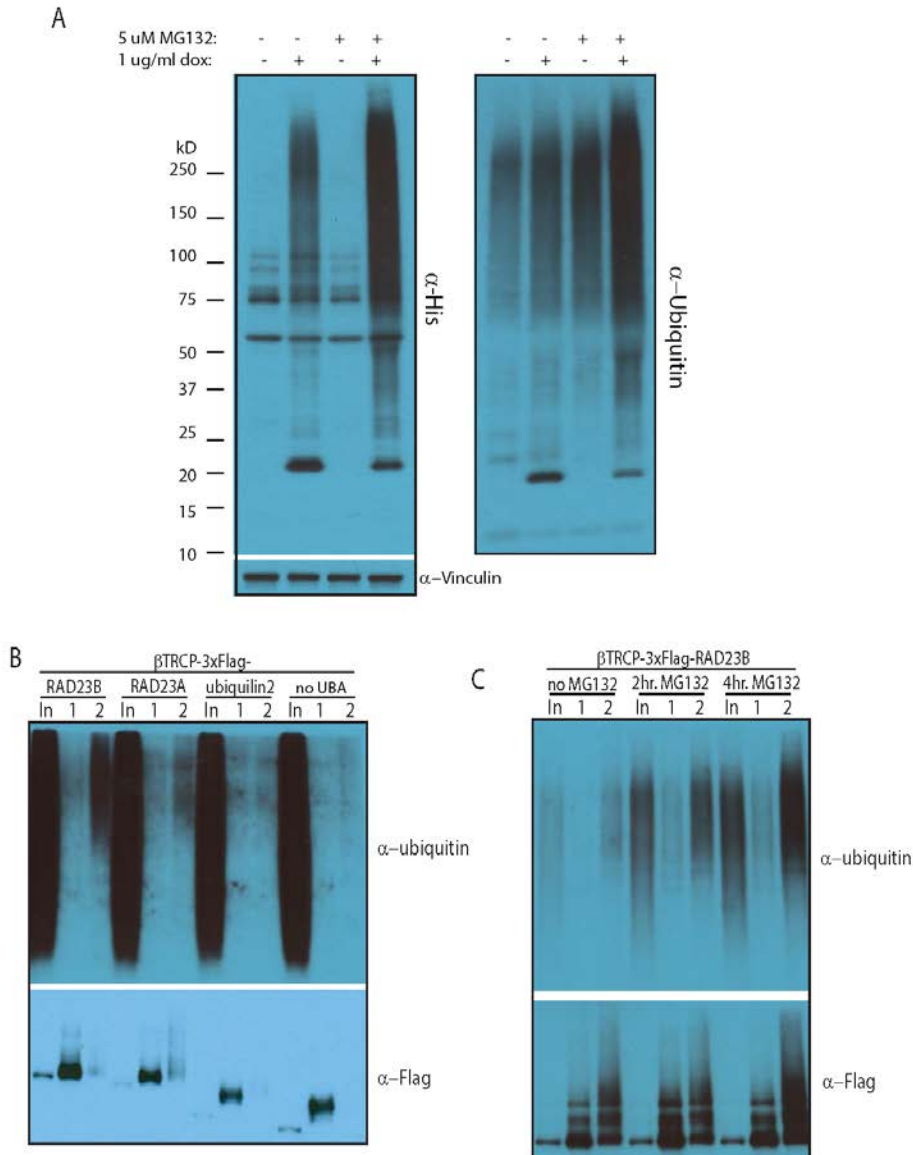


Fig 6. Consequences of CReP turnover downstream of eIF2 α phosphorylation. (A) UV dominantly prevents the induction of GADD34. 293 cells were treated with 300 J/m² UV-C, 1 μ M thapsigargin, or a combination of the two, and with 1 μ M MLN4924 where indicated. All treatments were added simultaneously. (B) CReP turnover reduces bulk translation after DNA

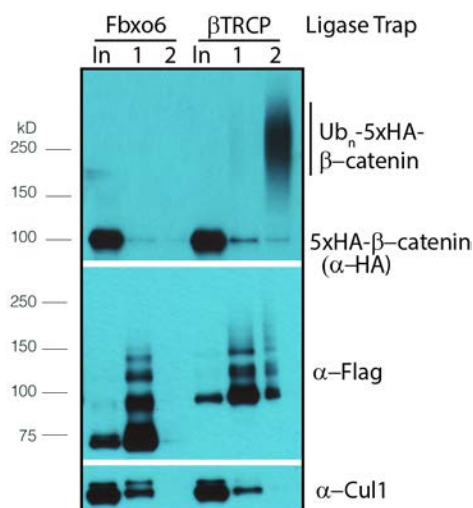
damage. HEK293 cells were transfected with plasmids expressing GFP, wildtype CReP, or stable mutant CReP^{31A}, then, as indicated, were untreated, treated with 1 µg/mL camptothecin (CPT) for 4 hours, or treated with CPT and then washed in medium to initiate DNA damage recovery for the indicated time. 10 minutes before collection, puromycin was added to cells at a final concentration of 10 µg/mL to label nascent polypeptide chains, and cells were collected in cold PBS, on ice, before flash-freezing. (C) Quantitation of (B) by densitometry. (D) A model for the role of CRLs in regulating eIF2α after DNA damage.

Supporting Information Captions



S1 Fig. Development of the mammalian Ligase Trapping protocol. (A) We created the 293 HisUb cell line, which expresses high levels of 6xHis-tagged ubiquitin upon doxycycline treatment, in addition to endogenous ubiquitin. We added doxycycline for 3 days and the proteasome inhibitor MG132 for 4 hours, where noted. (B) To choose a UBA domain to include in our Ligase Trap constructs, we fused UBA domains from 3 different sources to β TRCP. Cells were induced to express 6xHisUb with doxycycline, then transiently transfected with equal amounts of Ligase Trap constructs including β TRCP-3xFlag fused to the tandem UBA domains

of RAD23B or RAD23A, the single UBA domain of ubiquitin 2, or Flag alone, and the total 6xHisUb pulled down by each construct was assayed. Cells were treated with 5 μ M MG132 for 4 hours before lysis. The F box fusions were purified under native conditions with anti-Flag antibody and eluted with Flag peptide. Then, the eluate was denatured in 6M urea and ubiquitinated proteins purified with NiNTA beads and eluted with imidazole. Loading was 1X for input, 23X for the 1st step, and 195X for the 2nd step. (C) To determine the best course of MG132 treatment, we induced 6xHisUb expression and treated the stable cell line expressing the β TRCP-3xFlag-RAD23B Ligase Trap construct with 5 μ M MG132 for 0, 2, or 4 hours before lysis. Loading was 1X for input, 20X for the 1st step, and for the 2nd step, 936X for the α -ubiquitin blot and 312X for the α -Flag blot.



S2 Fig. Purification of ubiquitinated β -catenin by the β TRCP Ligase Trap. Stable cell lines expressing the β TRCP Ligase Trap or a negative control (FBXO6) were induced to express 6xHisUb for 3 days, transfected with 5xHA-tagged β -catenin for 24 hours, lysed and subjected to a two-step precipitation. First, the Ligase Traps were purified under native conditions with anti-Flag antibody and eluted with Flag peptide. Then, the eluate was denatured in 6M urea and ubiquitinated proteins purified with NiNTA beads and eluted with imidazole. Loading was 1X input (In), 160X 1st step (1), and 1950 2nd step (2) for the α -HA blot and 1X input, 20X 1st step, and 170X 2nd step for the α -Flag and α -Cul1 blots.

HIVEP1/2

Human DSGESEEE
Mus musculus DSGESDEE
Gallus gallus ESGESEDE

CReP

Human DDGFDS
Mus musculus DDGFDS
Gallus gallus DDGFDE

UBE4B

Human DTTFLD
Mus musculus DTTFLD
Gallus gallus DTTFLD

ZNF395

Human DSGSSTTS
Mus musculus DSGSSGHW
Gallus gallus DSGSSTTS

ZNF704

Human DDGIDEAE/SDGEED
Mus musculus DDGIDEAD/SDGEED
Gallus gallus DDGIDEAE/SDGEED

BAT2

Human DSGGSSE/DSGVDLS/DSGHCVPE
Mus musculus DSGGSSE/DSGVDLS/GSGQCVPE
Gallus gallus -----/DSGIDL/-----

SUN2

Human DDGSSSS
Mus musculus NDGSSSS
Gallus gallus EDGSSS-

AEBP2

Human SDGEPLS
Mus musculus SDGEPLS
Gallus gallus SDGEPLS

GGNBP2

Human DSGKGAKS
Mus musculus DSGKGAKS
Gallus gallus DTGKGAKS

ALDH2

Human DGDFFSYT
Mus musculus DGDFFSYT
Gallus gallus DGDFFCYT

TRIM9

Human DSGYGS
Mus musculus DSGYGS
Gallus gallus --GYGS

CEP44

Human SSGKSE
Mus musculus VSEKPE
Gallus gallus RPSKRE

DACT1

Human SSGFYELS
Mus musculus SSGFYELS
Gallus gallus SSGFYELS

FNIP1

Human DSGIARS
Mus musculus DSGIARS
Gallus gallus DSGIARS

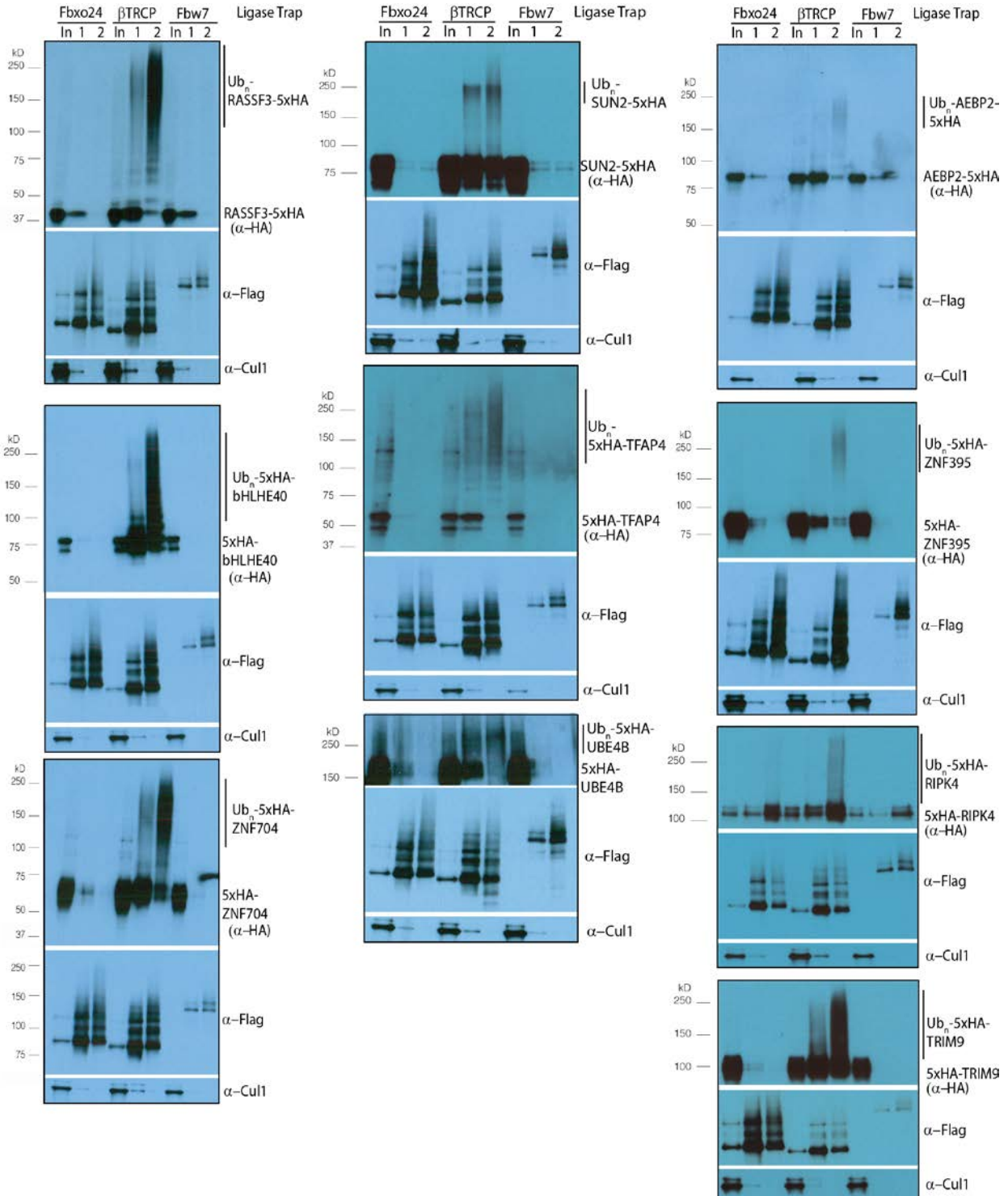
RIPK4

Human DSGAS
Mus musculus DSSAS
Gallus gallus DGNSS

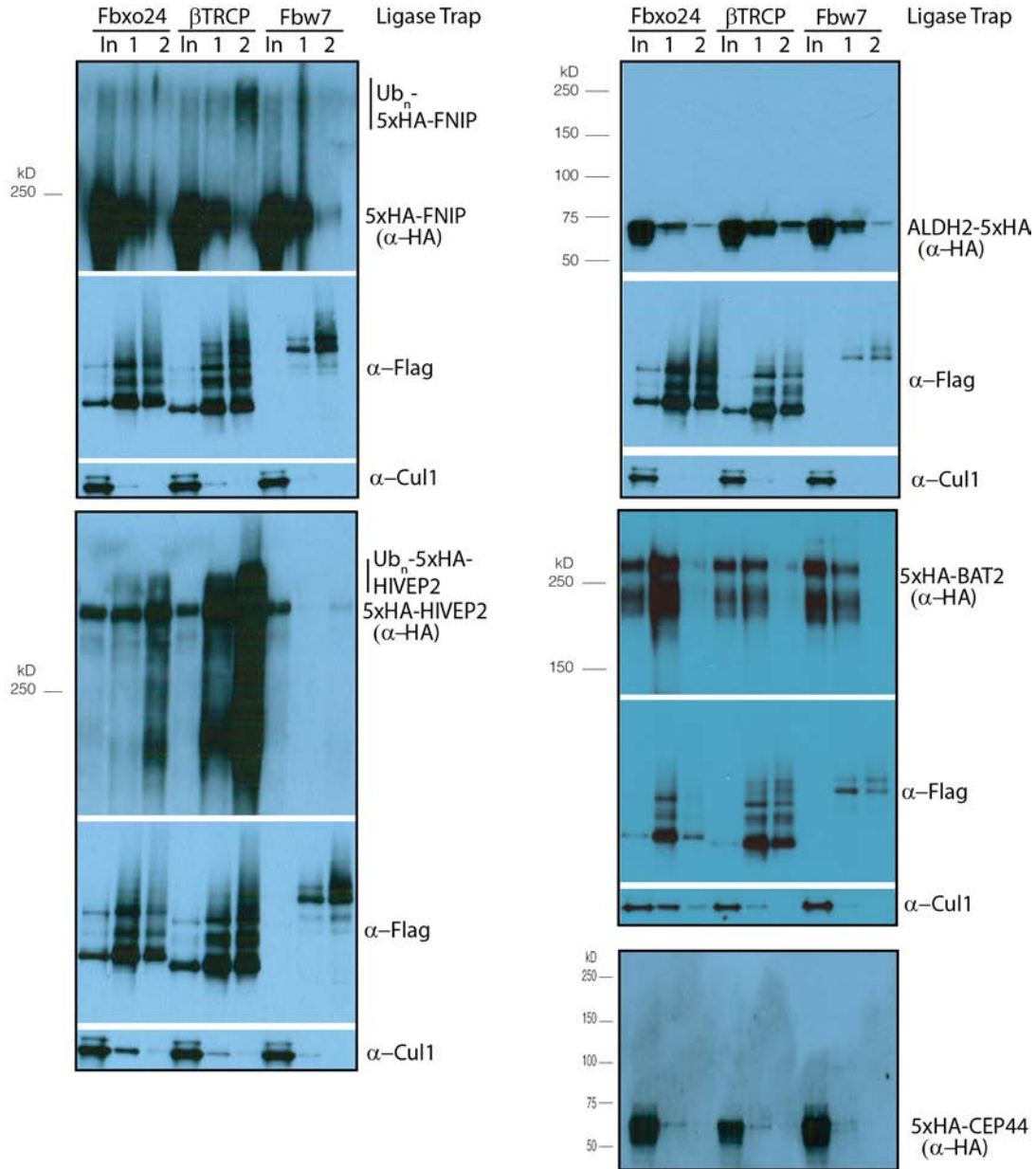
RASSF3

Human SSGYSS
Mus musculus SSGYSS
Gallus gallus SSGYCS

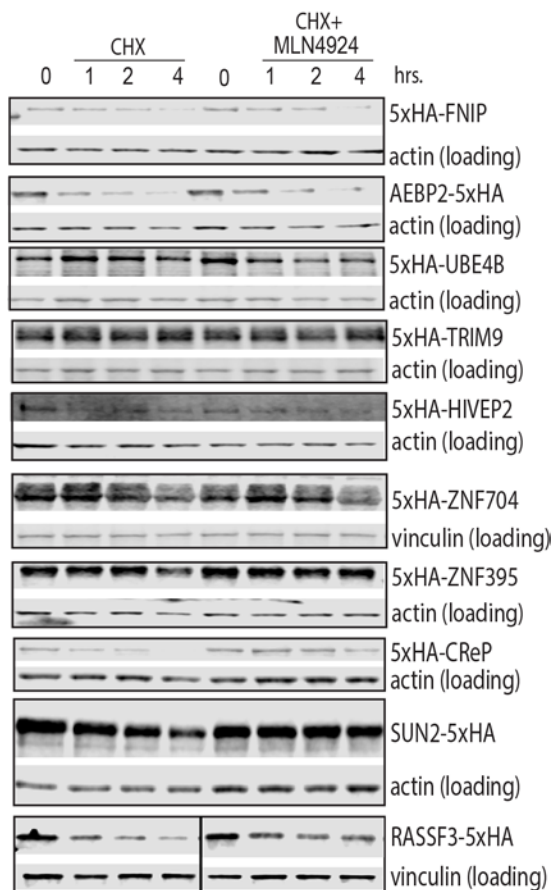
S3 Fig. Conservation of degrons observed in candidate β TRCP substrates. Comparison of degron sequences observed to the corresponding sequence in the mouse and chicken homolog.



S4 Fig. Pulldown of ubiquitinated species of candidate substrates by the β TRCP Ligase Trap. Complete IP results for candidate substrates shown in Fig 4, as well as for bHLHE40 and TFAP4, which are now listed as known substrates since they were published during the preparation of this manuscript.



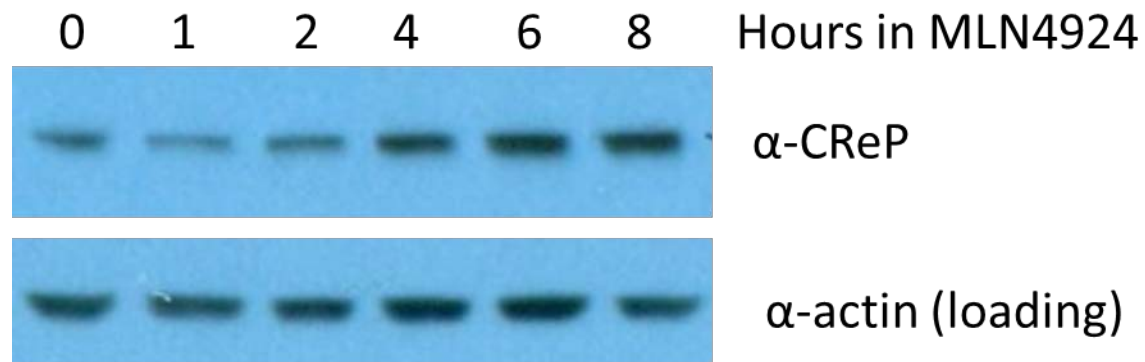
S5 Fig. Pulldown of ubiquitinated species of candidate substrates by the β TRCP Ligase Trap. As in Fig 4.



S6 Fig. Determination of candidate substrate stability and effect of SCF inhibition. Effect of SCF inhibition on candidate substrate half-life. 293 cells were transiently transfected with 5xHA-tagged candidate substrates and then treated with 100 $\mu\text{g}/\text{mL}$ cycloheximide (CHX) for the indicated time to halt protein synthesis. Where indicated, 1 μM MLN4924 was added at the same time as CHX. RASSF3 samples were all from the same blot and exposure.

Candidate Substrate	Average in MG132	no MG132 TSC1	no MG132 TSC2
Nrf2	11.7	0	0
CReP	12	0	0
UBE4B	15	23	23
ATF-4	13	0	0
CDC25A	10.7	0	4
ZNF395	8.7	0	0
HIVEP1/2 #	27.3	134	64
ZNF704	6.3	0	0
PDCD4	4.3	11	9
bHLHE40	7	3	2
CDC25B	5	0	2
BAT2	3.7	3	3
Deptor	4	0	0
SUN2 #	2	0	0
AEBP2	3	0	4
RAPGEF2	2.7	0	0
GGNBP2	2	0	5
TFAP4	2	2	4
Emi1	1	0	0
Per2	1.7	0	0
ALDH2	2.3	6	0
WWTR1	1.3	2	0
TRIM9 #	1.3	2	0
CEP44	0.7	0	0
DACT1	0.7	0	0
FNIP1	0.7	0	0
RIPK4	1.3	2	3
RASSF3	1	0	0

S7 Fig. Effect of MG132 on β TRCP Ligase Trap pulldowns. All substrates listed in Table 1 are included, with their average total spectral counts from three purifications in the presence of 5 μ M MG132 and two purifications in the absence of MG132.



S8 Fig. Accumulation of CReP upon CRL inhibition. HEK293 cells were treated with 1 μ M MLN4924 for the indicated time, and CReP levels assayed.

A

```

1  MEPGTGGSRRKRLGPRAGFRF
21 WPPFFRRSQAGSSKFPTPL
41 GPENSGNPTLLSSAQPETRV
61 SYWTKLSQLLAPLPGLLQK
81 VLIWSQLFGGMFPTRWLDFA
101 GVYSALRALKGREKPAAPTA
121 QKLSLSQLDSSDPSVTSPL
141 DWLEEGIHQWYSPDLKLEL
161 KAKGSALDPAQAFLLEQQ
181 WGVLLPSSLQSRLYSNREL
201 GSPSGPLNIQRIDNFSVVS
221 YLLNPSYLDVCFRLEVSYQN
241 SDGNSEVVGQTLTPESSCV
261 REDHCHPQPLSAELIPASWQ
281 GCPLSTEGLEIHLRMKR
301 LEFLQASKGQDLPTDQDN
321 GYHSLEEEHLLRMDPKHCR
341 DNPTQVPAAGDIPGNTQES
361 TEEKIELLTVPLALEEES
381 PSEGCPSSEIPMEKEPGEGR
401 ISVVDYSYLEGDLPIARPA
421 CSNKLIDYILGGASDLETS
441 SDPEGEDWDEAEADGDFDSD
461 SLSDDLEQDPEGLHLWNS
481 FCSVDYPNQNFATIQTAA
501 RIVPEEPDSEKDLGSKSDL
521 ENSSQSGSLPETPEHSSGEE
541 DDWESSADEAESLKLWNSFC
561 NSDDPNPLNFKAPFQTSGE
581 NEKGRDSTPSESIVAISE
601 CHTLLSCKVQLLGSQESECP
621 DSVQRDLVSGGRHTHVKRKK
641 VTFLEEVTEYISGDEDRKG
661 PWEEFARDGCRFQRIQETE
681 DAIGYCLTFEHRERMFNRLQ
701 GTCFKGLNVLKQC*

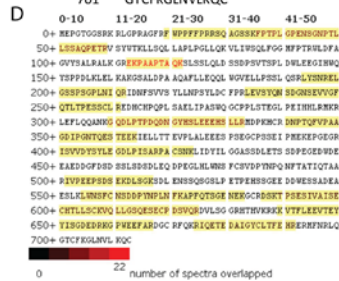
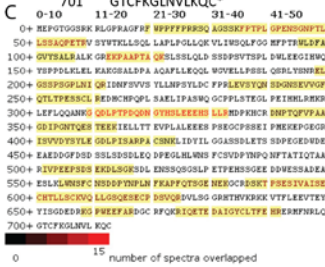
```

B

```

1  MEPGTGGSRRKRLGPRAGFRF
21 WPPFFRRSQAGSSKFPTPL
41 GPENSGNPTLLSSAQPETRV
61 SYWTKLSQLLAPLPGLLQK
81 VLIWSQLFGGMFPTRWLDFA
101 GVYSALRALKGREKPAAPTA
121 QKLSLSQLDSSDPSVTSPL
141 DWLEEGIHQWYSPDLKLEL
161 KAKGSALDPAQAFLLEQQ
181 WGVLLPSSLQSRLYSNREL
201 GSPSGPLNIQRIDNFSVVS
221 YLLNPSYLDVCFRLEVSYQN
241 SDGNSEVVGQTLTPESSCV
261 REDHCHPQPLSAELIPASWQ
281 GCPLSTEGLEIHLRMKR
301 LEFLQASKGQDLPTDQDN
321 GYHSLEEEHLLRMDPKHCR
341 DNPTQVPAAGDIPGNTQES
361 TEEKIELLTVPLALEEES
381 PSEGCPSSEIPMEKEPGEGR
401 ISVVDYSYLEGDLPIARPA
421 CSNKLIDYILGGASDLETS
441 SDPEGEDWDEAEADGDFDSD
461 SLSDDLEQDPEGLHLWNS
481 FCSVDYPNQNFATIQTAA
501 RIVPEEPDSEKDLGSKSDL
521 ENSSQSGSLPETPEHSSGEE
541 DDWESSADEAESLKLWNSFC
561 NSDDPNPLNFKAPFQTSGE
581 NEKGRDSTPSESIVAISE
601 CHTLLSCKVQLLGSQESECP
621 DSVQRDLVSGGRHTHVKRKK
641 VTFLEEVTEYISGDEDRKG
661 PWEEFARDGCRFQRIQETE
681 DAIGYCLTFEHRERMFNRLQ
701 GTCFKGLNVLKQC*

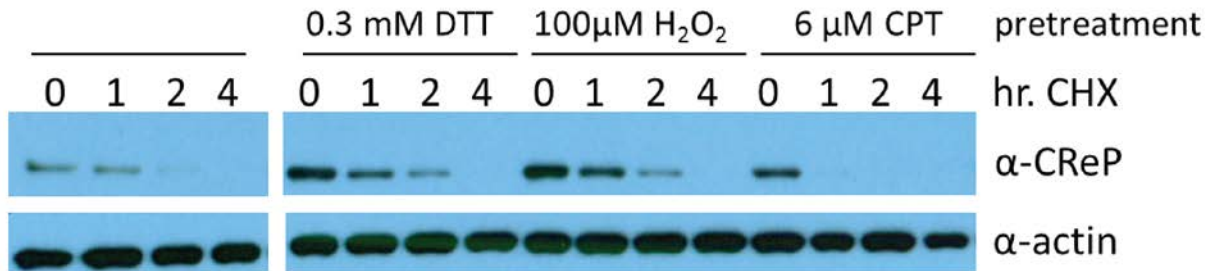
```



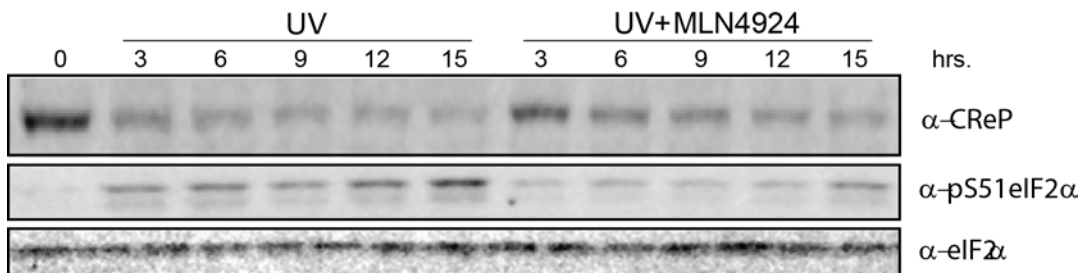
S9 Fig. Phospho-site mapping of CReP. 3xFlag-CReP was transiently expressed in 293 FlpInTRex cells, which were treated with 1 μ M MLN4924 for 5 hours and, where noted, 3 μ g/mL camptothecin for 4 hours before lysis. Then 3xFlag-CReP was purified with anti-Flag antibody, run on an SDS-PAGE gel, stained with colloidal Coomassie, and a band of the corresponding molecular weight was cut out. The gel slice was analyzed by mass spectrometry to identify phospho-sites. Predicted phospho-sites are shown for unstressed (A) and camptothecin-treated (B) cells. Coverage for unstressed (C) and camptothecin-treated (D) samples was about 40%.

1 MEPGTGGSRKRLGPRAGFRF
21 WPPFFPRRSQAGSSKFPTPL
41 GPENSGNPTLLSSAQPETRV
61 SYWTKLLSPLLAPLPGLLQK
81 VLIWSQLFGGMFPTRWLDFA
101 GVYSALRALKGREKPAAPTA
121 QKSLSSLQLDSSDPSVTSP
141 DWLEEGIHWQYSPDLKLEL
161 KAKGSALDPAAQAFLEQQL
181 WGVELLPSSLQSRLYSNREL
201 GSSPSGPLNIQRIDNFSVVS
221 YLLNPSYLDCFPRLEVSQYQ
241 SDGNSEVVGFTLTPESSCV
261 REDHCHPQPLSAELIPASWQ
281 GCPPLSTEGLEIHHLRMKR
301 LEFLQQASKGQDLPTPDQDN
321 GYHSLEEEHSLLRMDPKHCR
341 DNPTQFVPAAGDIPGNTQES
361 TEEKIELLTTEVPLALEEES
381 PSEGCPSEIPMEKEPGEGR
401 ISVVDYSYLEGDLPI SARPA
421 CSNKLIDYILGGASSDLETS
441 SDPEGEDWDEEAEDDGFDS
461 SSLSDSLEQDPEGLHLWNS
481 FCSVDPYNPQNFTATIQTAA
501 RIVPEEPSDSEKDLGKSDL
521 ENSSQSGSLPETPEHSSGEE
541 DDWESSADEAESLKLWNSFC
561 NSDDPYNPLNFKAPFQTSGE
581 NEKGCRDSKTPSESIVAISE
601 CHTLLSCKVQLLGSQESECP
621 DSVQRDVLGGRRHTHVKKR
641 VTFLEEVTEYYISGDEDRKG
661 PWEEFARDGCRFQKRIQETE
681 DAIGYCLTFEHRERMFNRLQ
701 GTCFKGLNVLKQC*

S10 Fig. Amino acid sequence of CReP, with stabilizing mutations marked. Residues mutated to alanine in the 11A mutant are marked in red. The 31A mutant includes those alanines as well as alanines in place of the residues marked in blue.



S11 Fig. DNA damage decreases CReP half-life. Cells were treated with the indicated concentrations of the indicated drugs for 2.5 hours before addition of cycloheximide for the indicated time.



S12 Fig. CRL activity is required for full CReP depletion and eIF2 α phosphorylation after UV treatment in mouse embryonic fibroblasts (MEFs). Immortalized MEFs were treated with 300 J/m² UV-C light for the indicated time, and simultaneously with 1 μ M MLN4924 where indicated.

Publishing Agreement

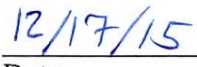
It is the policy of the University to encourage the distribution of all theses, dissertations, and manuscripts. Copies of all UCSF theses, dissertations, and manuscripts will be routed to the library via the Graduate Division. The library will make all theses, dissertations, and manuscripts accessible to the public and will preserve these to the best of their abilities, in perpetuity.

Please sign the following statement:

I hereby grant permission to the Graduate Division of the University of California, San Francisco to release copies of my thesis, dissertation, or manuscript to the Campus Library to provide access and preservation, in whole or in part, in perpetuity.



Author Signature



Date